Wireless Charger for Hand-held Mobile Devices

EE3L11 - BSc Project: Final Thesis

July 6, 2018

N. Toth
J. van der Horst

Technische Universiteit Delft

TU Delft Delft University of Technology

Challenge the future

WIRELESS CHARGER FOR HAND-HELD MOBILE DEVICES

EE3L11 - BSC PROJECT: FINAL THESIS

JULY 6, 2018

by

N. Toth
J. van der Horst

in partial fulfillment of the requirements for the degree of

Bachelor of Science
in Electrical Engineering

at the Delft University of Technology,
to be defended publicly on Monday July 2, 2017 at 11:00 AM.

Supervisor:	dr. M. Babaie	
Thesis committee:	Prof. dr. P. M. Sarro,	TU Delft
	Ir. F. van der Zwan	TU Delft
	Ir. M. J. Pelk	TU Delft
	dr. S. M. Alavi	TU Delft

This thesis is confidential and cannot be made public until July 1, 2023.

TU Delft Delft University of Technology

ABSTRACT

In recent years the field of wireless charging has seen remarkable developments. More and more devices like mobile phones and laptops can be charged wirelessly, and larger equipment like electric vehicles are likely to follow the same path. The air gaps over which the power can be transferred keeps increasing, as do the amount of power that can be transferred and the power transfer efficiency. Though combining these three key requirements has turned out to be a problem, since there always seems to be a trade off. This thesis will focus on the design process and the result of a wireless charger for hand held devices like mobile phones. This thesis will only describe the receiver side of the wireless power transfer system. The requirements were an output of 5V at 5W, over an as large as possible air gap with an efficiency of at least 60%. After the complete circuit had been designed and assembled an efficiency of 67.8% at a distance of 2.5cm had been obtained, which satisfies the requirements.

PREFACE

The authors, Nandor Toth and Jordy van der Horst, have written this document as part of their thesis for their Bachelor Graduation Project 'A Wireless Charger for Hand-held Mobile Devices' for the degree of Bachelor of Science in Electrical Engineering at Delft University of Technology. It was commissioned by the ELCA research group of the Microelectronics Department at the faculty of Electrical Engineering, Mathematics and Computer Science (EEMCS).

The report documents the 8 weeks that were spent developing a wireless charger for hand-held mobile devices with a transfer efficiency of at least 60% combined with a maximum physical distance between the transmitting and receiving sides of this charging unit. This report describes the principle of operation, the design process and the trade offs that lead to the final product of the receiving side together with the coil implementation. The design of the transmitting side is done by two other students, Joram van der Velden and Louis Marting, and will be treated in a separate thesis. [1]

We would like to thank Martin Schumacher and Xavier van Rijnsoever for their advice and guidance during our lab sessions. Special thanks goes out to Morteza Alavi, Marco Pelk and Masoud Babaie for making this project available and for assisting us during the project process.

N. Toth
J. van der Horst
Delft, July 6, 2018

CONTENTS

1

INTRODUCTION

Wireless power transfer (WPT) is slowly taking over charging of hand-held mobile devices, even larger equipment like electric cars are following. Attributes like power transfer distance and power efficiency have kept increasing the past decade. The number of possibilities are endless and still in the first phase of development. WPT uses an electromagnetic field created by a transmitter device to transfer electrical energy over a certain distance to the receiver, which is capable of extracting power from this field and supplying it to a load. The goal is to design a high efficiency WPT-system with an 5 watt output.

1.1. STATE-OF-THE-ART ANALYSIS

There are two main techniques used in WPT-systems, far-field (radiative) power transfer and near-field (non-radiative) power transfer [2].
Far field power transfer uses visible light or microwaves to transfer power from the transmitter to the receiver. Radiative power transfer often achieves power transfer over larger distances than non-radiative power transfer, but obtains a poorer efficiency.

Non-radiative resonant inductive coupling has multiple current and/or possible future applications, they differ from high to low power wireless charging. The automotive industry is putting a lot of effort in high power wireless charging. The first cars that use wireless charging are already available. The medical industry is also investing in low power systems to charge bio medical implants[3]. However hand-held mobile devices provide by far the biggest market and have been common for quite some time now. With wireless charging a device can be fully sealed, allowing it to be fully water proof. The lack of cables also promises a better longevity[2].
The most efficient way to transfer power wirelessly is to do it via a standard, so that the transmitter and receiver can communicate properly. A widely adopted wireless power transfer standard is the Qi standard[4] [5], developed by the Wireless Power Consortium (WPC) in 2009. This standard uses a back and forth communication between the receiver and the transmitter, so that the right amount of power is transmitted at the right frequency at all times. The number of products that are currently compatible with Qi is over 1600. Qi operates in a frequency range between 80 and 200 kHz and can deliver between 2W and 2000W depending on the device. The efficiencies of such systems lies around 60-70% at a transfer distance of around 1 to 3cm.
Another lesser known and adopted wireless power transfer standard is Airfuel Resonant [6] developed by the Airfuel alliance in 2015. This standard can achieve higher distances than Qi and operates at a larger frequency in the range of MHz.

1.2. PROBLEM DEFINITION

Wireless charging is nowadays conventional in many hand-held mobile devices. But the charging methods used in systems today are far from perfect. Some disadvantages like the power transfer efficiency and distance for delivering power still need to be improved [7]. Efficiency's almost as high as wired charging is achievable, however the major drawback of this technique is the size of the coils. The size is not scalable and will never fit on the back of a mobile phone. With regular sized coils the power efficiency and transfer distance are limited. Other phenomena like misalignment of the coils [8] in combination with the variation of the coupling

and power delivered form huge problems for efficiency and steady output power. A small difference in coil alignment, a mismatched load or a different coupling results in a large drop in efficiency. Wireless power charging systems are therefore still not completely ideal to use.

1.2.1. THE BASIC PRINCIPLE

The basic principle on which a wireless power transfer system relies is given by Faraday's law. Faraday's law states that a changing magnetic field within a wire loop (the magnetic flux) will induce voltage called the electromotive force (EMF), as can be seen in formula 1.1. [9].

$$EMF = -\frac{d\phi_B}{dt} \tag{1.1}$$

A primary coil turns the electric AC power of the transmitter into a time-varying magnetic field. The flux of this magnetic field flows through the secondary coil in the receiver, which turns the magnetic field back into electric AC power. In order to transfer enough power, the EMF must be high enough. Therefore, the change of the magnetic flux variation must be high or the amplitude of the flux captured must be greater. In formula 1.1 it can be seen that the magnetic field gets larger as the variation in flux over time gets larger. This works the other way around as well. In order to get the flux variation in time as large as possible, the frequency should be high (lowering dt) or by enlarging the EMF. A way that the EMF can be made larger, is by letting the voltage oscillate in a resonant circuit containing a capacitor in series with the coil [10]. This principal will be explained further later in this thesis.

The circuit implementing this basic principle is as follows. An inverter produces the AC voltage that powers the primary coil. How much flux of the propagated magnetic field is absorbed by the secondary coil is determined by the coupling coefficient. This coupling coefficient is determined by the distance between the coils and by how well the coils are aligned [11]. The receiver converts the delivered AC power into DC power and ensures a constant power over the load of the desired magnitude [12][13]. A schematic of this basic circuit is shown in the figure below.

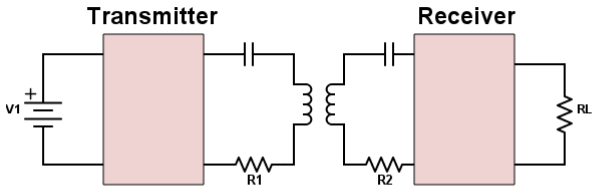

Figure 1.1: Basic resonating circuit for wireless power transfer

In this circuit, V_{in} is the transmitter, R_L is the receiver, and the components in between are the coupled LC-circuits with their internal resistances R_1 and R_2. This basic circuit already addresses a limitations that the system must adhere to. The receiver coil must be in the range of the transmitting field and the coils must be properly aligned. Together with the frequency- and high voltage requirement caused by the basic principle described in Equation 1.1, these form the constraints of the system. Within these constraints the main objective is to reduce losses[14].

1.3. SYNOPSIS

The outline of the thesis is as follows. To design the receiver of a wireless power transfer system. The system should at least be 60% efficient and deliver 5W at 5V. The system is meant for hand-held mobile devices. Furthermore, possible ways of increasing the distance between the coils should be examined.

2

PROGRAMME OF REQUIREMENTS

The main goal of this bachelor project is to implement a wireless charger circuit. As stated before, this project is separated into two main parts: The transmitting side and the receiving side. The receiving side combined with the air coupled coils will be discussed in this report. The requirements follow from the full system requirements:

1. Wireless power transfer protocol: preferably Qi, the frequency of operation need to be around 80-300 kHz;
2. Transfer efficiency: as high as possible, but at least around 60%;
3. Transmitting side (TX) output power: around 5-10W;
4. Receiving side (RX) output power: around 5W;
5. Physical distance between TX and RX as high as possible;

The complete system requirements provide a guidance for the requirements of each separate part of this wireless power transfer circuit.

2.1. FUNCTIONAL REQUIREMENTS

1. The system should convert the AC input signal delivered by the receiver coil into a DC signal;
2. The system will have a fixed output voltage and power;
3. The output values should be achieved at an as large as possible range of distances;
4. The power efficiency should be as high as possible;

2.2. ENVIRONMENTAL REQUIREMENTS

1. The transmitter frequency, bandwidth and output power must fall within Dutch regulations;
2. The product must function indoor and outdoor;

2.3. SYSTEM REQUIREMENTS

1. A proper magnetically coupled inductor to collect the transmitted electromagnetic signal must be designed;
2. The oscillation frequencies of the transmitter and the receiver need to be the same;
3. The oscillation frequency received by the receiver coil should be between 80 and 300 kHz;
4. A low loss rectifier must be designed;

5. A voltage control unit must be designed to deliver a fixed 5W at 5V output;
6. The efficiency of the entire system containing transmitter, coils must exceed 60%;
7. The efficiency of the receiver must exceed 85%;
8. The ripple in the output may not exceed 2%;
9. The product's width should not exceed 5cm, the length and height must be as small as possible;

2.4. INSTALLATION REQUIREMENTS

1. The product should be easily implementable to hand-held devices

3

DESIGN

The full system consists of two main elements: The transmitter and the receiver. These two elements are connected through two air coupled coils. Figure 3.1 shows a simple block diagram with the elements that will be discussed in this chapter. The transmitter, which is part of another project [1], delivers a square wave to coil L1. The next step is a full-bridge rectifier to convert the received alternative time-varying signal to a constant voltage. Because the physical distance between coil L1 and L2 will vary, the magnitude of the output voltage will be variable. A voltage regulator is designed to keep a constant 5V output suitable for hand-held mobile devices.

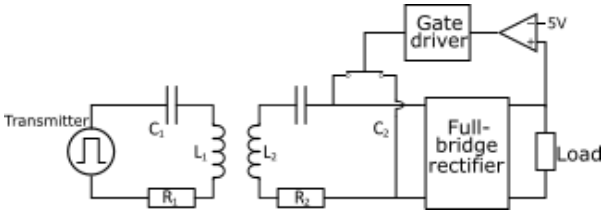

Figure 3.1: Functional block diagram of the receiver

A detailed description of the design choices and the final full circuit will be discussed in this chapter.

3.1. RESONANT CIRCUIT

As stated in the introduction, wireless power transfer relies on the fact that two coupled coils can transfer energy, more formally described by Faraday's law. Faraday's law states that a changing magnetic flux through a surface bounded by a wire will induce an electromotive force. The magnitude and difference in time of this flux determine how much energy can be transferred.

3.1.1. RESONANT CIRCUIT REQUIREMENTS

The resonant circuit has to meet the following requirements:

1. The voltages have to be as large as possible in order to create an as large as possible flux.
2. The components must be able to handle the induced voltages.
3. The circuit losses should be as small as possible

3.1.2. CIRCUIT THEORY

Calculating the flux the two coils share requires sophisticated modelling of the fields. A more practical approach comes from circuit theory. In circuit theory, two coupled coils are shown as a two-port. Figure 3.2 shows a two-port with coils L_1 and L_2.

The relations between the phasor voltages and currents for the coils in Figure 3.2 are given as follows:

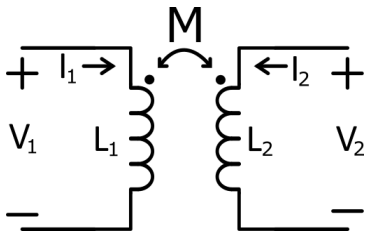

Figure 3.2: Two-port network of coupled coils

$$\begin{aligned} \mathbf{V_1} &= j\omega L_1 \cdot \mathbf{I_1} + j\omega M \cdot \mathbf{I_2} \\ \mathbf{V_2} &= j\omega M \cdot \mathbf{I_1} + j\omega L_2 \cdot \mathbf{I_2} \end{aligned} \tag{3.1}$$

Where the mutual inductance M is defined as:

$$M = k\sqrt{L_1 L_2}, \quad 0 \leq k \leq 1 \tag{3.2}$$

The mutual inductance M is a measure for how much electromotive force $\mathscr{E}$ is induced at a certain coupling factor k. k therefore defines the amount of the induced field that the coils can capture. For example, imagine that coil L_2 is connected to an open terminal, then Equation 3.1 is simplified to the following:

$$\begin{aligned} \mathbf{V_1} &= j\omega L_1 \cdot \mathbf{I_1} \\ \mathbf{V_2} &= j\omega M \cdot \mathbf{I_1} \end{aligned} \tag{3.3}$$

These formulas show the induced voltage V_2 at the second coil directly relates to the current through the first coil I_1 using the mutual inductance M. When k equals 1, the coupling M is at a maximum. At k is 0, there is no coupling and no power can be transferred.
The term omega (ω) is the angular frequency and is also a factor for the induced voltage. At a higher frequency the change in the magnetic field is increased, from Faraday's law follows that the induced voltage increases.

3.1.3. POWER TRANSFER

In a wireless power transfer system the coils can be placed relatively far apart. Therefore, the coupling is low ($k \approx 0.1$). However, the power transfer should still be more than 5 watts. As seen in the section above, the coupling between the coils and the angular frequency are both directly related to the induced voltage. The induced voltage powers the load. Thus, to increase power transfer the angular frequency and the coupling need to be maximized within the bounds of the system.

Firstly, the theoretical power transfer possible over the airgap should be defined. Starting from Equation 3.1, the phasor currents and voltages are defined. The power transferred is the real part of the apparent power through the system.

$$P = -\mathrm{Re}(\mathbf{V_2}\mathbf{I_2^*}) = \mathrm{Re}(\mathbf{V_1}\mathbf{I_1^*}) \tag{3.4}$$

This results in the real power defined as:

$$P = -\mathrm{Re}(j\omega M \cdot \mathbf{I_1} \cdot \mathbf{I_2^*}) \tag{3.5}$$

For maximum positive power transfer, there should be no reactance, i.e. the phase of the apparent power should be 0°. The minus in Equation 3.5 for the receiving side (due to current convention of a two-port) makes that the multiplication of $\mathbf{I_1}$ and $\mathbf{I_2^*}$ should have a phase of 180°.
The imaginary unit j adds a 90° shift to the multiplication of $\mathbf{I_1}$ and the complex conjugate $\mathbf{I_2^*}$, so the result of the multiplication should be 90°. The result is that $\mathbf{I_1}$ leads $\mathbf{I_2}$ with 90°. The power transfer now can be represented by a sine function of α, where α is the angle between $\mathbf{I_2}$ and $\mathbf{I_1}$.

$$P = \omega M \cdot I_1 \cdot I_2 \cdot \sin\alpha \quad [W] \tag{3.6}$$

I_1 and I_2 are the RMS values of the currents through the coils L_1 and L_2 respectively. The mutual inductance M and angular frequency ω are defined as previously stated. The requirement for $\alpha = 90°$ is satisfied in Section 3.1.4 using capacitors. Let us assume for now that this requirement has been met.

The system requirements state that the system should deliver 5 watts. The worst case within the specifications would be 60% efficiency at the load with 85% efficiency of the transmitter [1]. Assumed is that the transferring coils are loss-less and all power is transferred according to Equation 3.6. The minimal efficiency of the receiver must be 60%/85% = 71%. The power that is delivered through the air gap is therefore 5/71% = 7.1 watts.

3.1.4. TUNING CIRCUIT

In the previous section, α was determined to be 90° for maximum power transfer, with all other factors constant. To change the phase of $\mathbf{I_2}$ an impedance is required. The following constraint is added to Equation 3.1 for shifting the phase:

$$\mathbf{V_2} = -Z \cdot \mathbf{I_2} \tag{3.7}$$

The minus is due to the current defined as going in the two-port, and not through the load. Z is defined as $Z = R + X$. Adding Equation 3.7 to Equation 3.1 results in the following formula:

$$\mathbf{I_2} = \frac{j\omega M}{-Z - j\omega L_2} \cdot \mathbf{I_1} \tag{3.8}$$

For $\mathbf{I_2}$ to be 90° lagging, the reactance in the denominator must be cancelled. The term $j\omega M$ in combination with $-R$ will exactly shift the phase by 90°, this leaves us with the following constraint:

$$X = -j\omega L_2 \tag{3.9}$$

Let us use a capacitance for X_L to try to satisfy this formula.

$$\frac{1}{j\omega C_2} = -j\omega L_2 \tag{3.10}$$

This leaves us with the constraint:

$$\omega_0 = \frac{1}{\sqrt{L_2 C_2}} \tag{3.11}$$

This constraint is the same formula as for a resonant LC-circuit. The tuning capacitor C_2 must be chosen in such a way that the system is in resonance at the desired frequency. This will achieve maximum theoretical power transfer. The frequency behaviour of an LC circuit is shown in figure 3.3b.

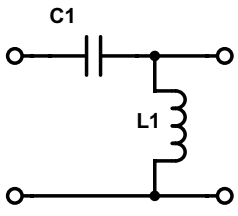

(a) LC resonant circuit two-port diagram

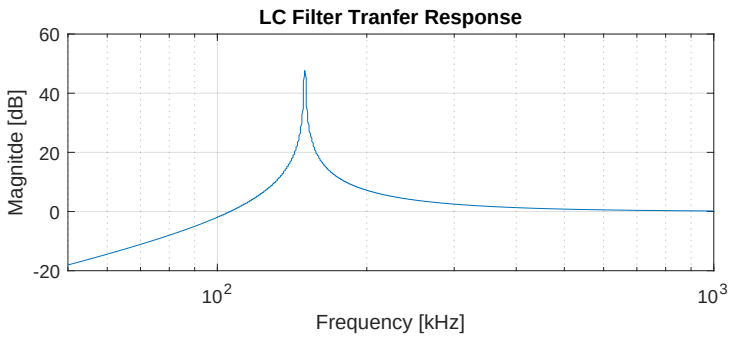

(b) Transfer function of the LC resonant circuit as seen in Figure 3.3a

Whether the tuning capacitor is in series or in parallel with the coil, will influence the behaviour of the circuit. In parallel the load resistance has influence on the oscillation frequency and the achieved frequency is poorer as can be seen in table I-IV in [15] however. For this reason, a series-series capacitor topology was chosen, as can be seen in figure 3.4.

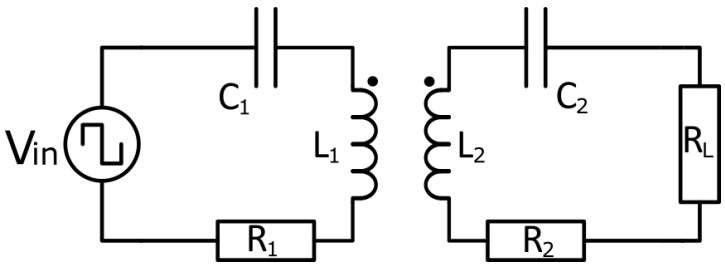

Figure 3.4: Series-series resonant circuit configuration

3.1.5. COIL DESIGN CONSIDERATIONS

Two important factors in the coil design are the coil inductance and the coil AC resistance. These two parameters are related by the quality factor (Q-factor) as stated in Equation 3.12.

$$Q = \frac{\omega \cdot L}{R} \tag{3.12}$$

The quality factor describes how under-damped a resonator or oscillator is. Resonators with a high quality factor have a larger amplitude at the resonant frequency, but they have a smaller range around that frequency for which they resonate [16]. A simple definition for the quality factor is the ratio between the energy stored in the resonator and the energy dissipated by the damping process. Which for electrical systems means: The ratio between the energy stored in inductors-and capacitors and the energy dissipated in resistors.
A bigger coil with a higher inductance is able to generate a stronger magnetic field. Thus a high inductance is desired. Also, a low resistance is desired as this will ensure that less power is lost when current flows through the coil. Therefore, the coil will have to have a high Q-factor. As assembling a coil requires very precise engineering, due to the possibility of gaps between the windings and pitch variation, it was decided to buy the coils from an external company. There are multiple options available, but it was found that only the coils of 'Würth Electronics' had an extensive amount of data in the datasheets, where mainly the Q-factor as a function of the frequency applied was very useful. Figure 3.5 shows this relationship.

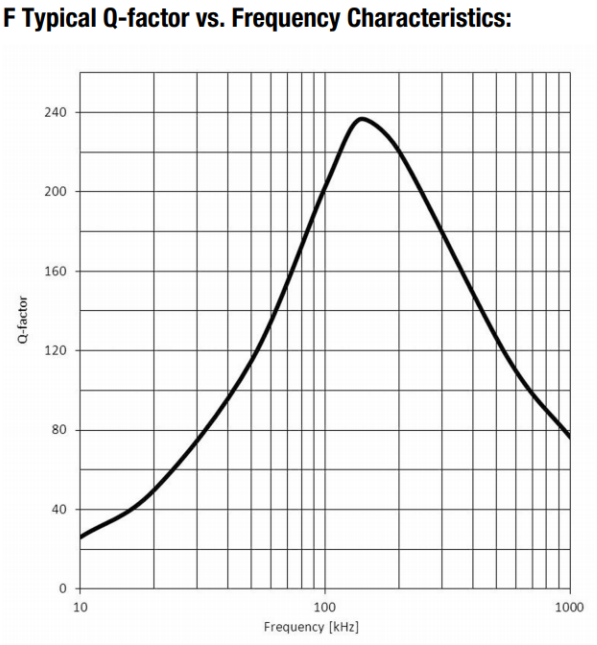

Figure 3.5: Q-factor as a function of the frequency applied [17]

This relationship is caused by two phenomena. The incline in Q-factor as the frequency rises (to 100 kHz) is caused by the linear relationship between Q and ω. The decline in Q-factor as the frequency rises (from 200 kHz) is caused by the skin effect in the Litz wire, which increases the AC resistance. As Q and R are inversely

proportional, the Q-factor will decrease as this skin effect begins to play a role. The frequency at which this happens is dependent on the diameter of the Litz wire that is used. These effects show that there will be an optimal operating frequency for the coil. However, the capacitor also has to be considered.

Skin Effect In conductors, the penetration of high-frequency signals is governed by the skin effect. This penetration is weaker within the conducting wire, thus the resistance in the inner part of the wire is larger, that of the outer part of the wire. The depth at which the penetration of the signal is significant is called the skin depth (δ) and is among other things dependent on the frequency. As the frequency rises, the skin depth becomes smaller, thus the total resistance of a piece of wire increases, as Equation 3.13 shows. [18]

$$R/R_{DC} = \frac{\pi \cdot r^2}{\pi \cdot (2 \cdot r - \delta) \cdot \delta} \quad with \quad \delta = \sqrt{\frac{2 \cdot \rho}{\omega \cdot \mu}} and r > \delta \tag{3.13}$$

This is why, for high-frequency coils, Litz wire is used. This Litz wire has lots of small strands of wires instead of one solid wire. These smaller strands have a much larger surface area and will thus have less resistance at high frequencies compared to normal wire. This is shown in Figure 3.6.

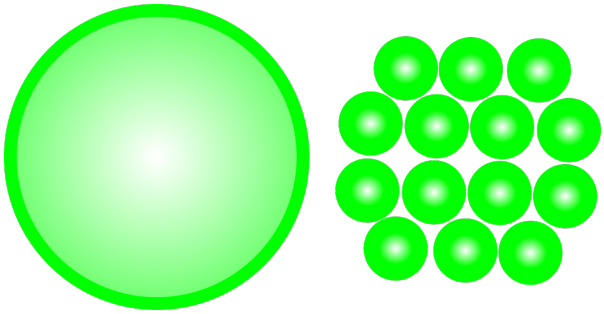

Figure 3.6: Illustration of the skin effect in Litz Wire

However, also in Litz Wire skin effect plays a role. This is seen in Figure 3.5. For a copper wire with a radius of $0.2mm$ this phenomena starts to effect the resistance around 150 kHz. This is shown in Figure 3.7

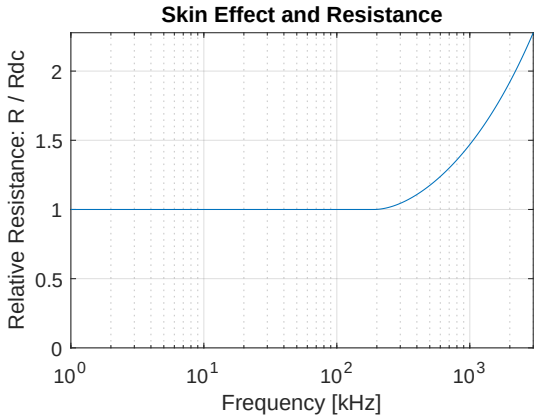

Figure 3.7: The resistance in Litz wire

A number of coils were considered, with the coil inductance and Q-factor in mind. The highest inductance and Q-factor was found in coil '760308110' from 'Würth Electronics' [17]. These coils have an inductance of 25.3 μH, measured using a LCR Meter HC8018.

3.1.6. CAPACITOR DESIGN CONSIDERATIONS

As efficiency is an important requirement, this also has to be considered when choosing one or multiple tuning capacitors. Ceramic capacitors will be used, because these can withstand both positive and negative voltages as opposed to electrolytic capacitors. The three most common type of dielectric material in ceramic

capacitors are X7R, Z5U and NP0. The difference in equivalent series resistance (ESR) between these two materials is significant. The dissipation factor (DF) of X7R and Z5U capacitors are generally above 1.5%, while NP0 capacitors generally have a dissipation factor below 0.1%. This is directly related to the ESR as seen in Equation 3.14. Also, X7R capacitors have a strong dependency of their voltage, causing the capacitance to drop at higher voltages. Furthermore, for NPO materials the dielectric constant remains constant up to about 1 GHz. Thus NP0-type dielectric ceramic capacitors will be used. [19]

$$ESR = \frac{DF}{\omega \cdot C} \tag{3.14}$$

3.1.7. OPERATING FREQUENCY OPTIMIZATION

There are several different frequency dependent elements in the design that make for a frequency dependent power loss and thus a frequency dependent efficiency. These are the amount of power that is transferred, the resistance of the coil and tuning capacitor and the losses in the control circuit. Therefore, an analysis has been done to optimize the operating frequency.

3.1.8. POWER TRANSFER INFLUENCES

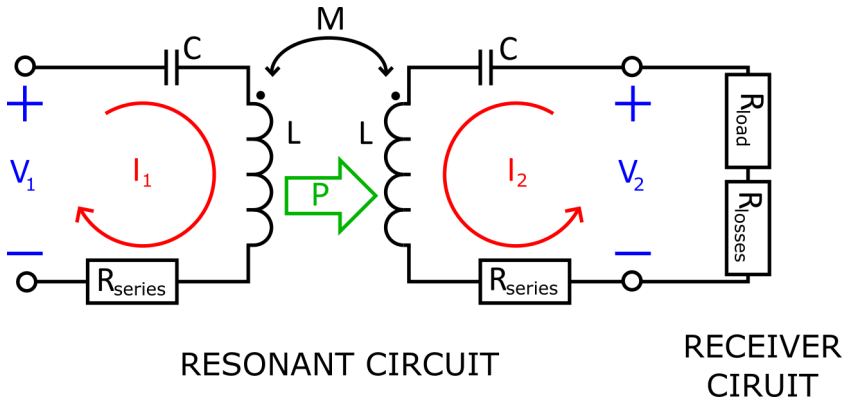

Figure 3.8: Power transfer in the resonant circuit

Firstly, the effect of the frequency on the transferred power in the circuit is discussed. The relationship between the power transferred and the frequency is described in Equation 3.15, where α is the phase angle between I_1 and I_2, which should be 90° (Section 3.1.3) [20].

$$P = \omega \cdot M \cdot I_1 \cdot I_2 \cdot sin(\alpha) \quad [W] \tag{3.15}$$

Important to note are the currents through the resonant circuits as these are related to the power loss in the equivalent series resistances of the components. In order to determine these losses, the currents through the components have to be known. The ratio between the current in the transmitter coil and the receiver coil is given in Equation 3.16. This has been derived from Equation 3.8 when Equation 3.11 holds.

$$|\mathbf{I_2}| = \frac{\omega M}{R} \cdot |\mathbf{I_1}| \quad \Rightarrow \quad I_2 = \frac{\omega M}{R} \cdot I_1 \quad [A] \quad with \quad R = R_{load} + R_{losses} + R_{series} \quad [\Omega] \tag{3.16}$$

R_{load} is the load that will be placed in the receiver circuit. This has a value of 5Ω. R_{losses} are the losses present in the receiver circuit, modelled as a resistance. As the efficiency of the receiver is assumed to be 90%, this resistance has a value of $\frac{5}{0.90} - 5 = 0.555\Omega$. The losses in the components of the receiving resonant circuit are modelled as an equivalent series resistance. For now this is given a resistive value of 0.1Ω, making up a total resistance of 5.655Ω.

With Equation 4.6 and Equation 3.16, a formula for the current through the transmitter resonant circuit can be obtained:

$$I_1 = \frac{P}{\omega M} \cdot \frac{1}{I_2} = \frac{P}{\omega M} \cdot \frac{R}{I_1 \cdot \omega M} = \frac{P \cdot R}{I_1 \cdot (\omega M)^2} \quad [A] \tag{3.17}$$

$$I_1^2 = \frac{P \cdot R}{(\omega M)^2} \quad \Rightarrow \quad I_1 = \frac{\sqrt{P \cdot R}}{\omega M} \quad [A] \tag{3.18}$$

Also, the current through the receiver can be obtained:

$$I_2 = \frac{\omega M}{R} \cdot I_1 = \frac{\omega M}{R} \cdot \frac{\sqrt{P \cdot R}}{\omega M} = \sqrt{\frac{P}{R}} \quad [A] \tag{3.19}$$

From this the power dissipated in the transmitter resonant circuit can be calculated:

$$P_{loss-1} = I_1^2 \cdot R_{series} = \frac{P \cdot R}{(\omega M)^2} \cdot R_{series} \quad [W] \tag{3.20}$$

$$P_{loss-2} = I_2^2 \cdot R_{series} = \frac{P}{R} \cdot R_{series} \quad [W] \tag{3.21}$$

$$P_{loss} = P_{loss-1} + P_{loss-2} = P \cdot \left(\frac{1}{R} + \frac{R}{(\omega M)^2} \right) \cdot R_{series} \quad [W] \tag{3.22}$$

The amount of power transferred should be the amount of power used by the load, the losses in the receiver and the losses in the receiving resonant circuit. Equation 3.23 shows that the RMS current through the receiving loop should be $1A$. This means that the power consumed by the load and losses is equal to their resistive values: $P = 5.655W$. ω is the operating and resonant frequency, M is the mutual inductance between both coils. This results in a power loss and efficiency as seen in Figure 3.9

$$P_{load} = I_{rms}^2 \cdot R_{load} \quad \Rightarrow \quad I_{rms} = \sqrt{\frac{P_{load}}{R_{load}}} = \sqrt{\frac{5}{5}} = 1[A] \tag{3.23}$$

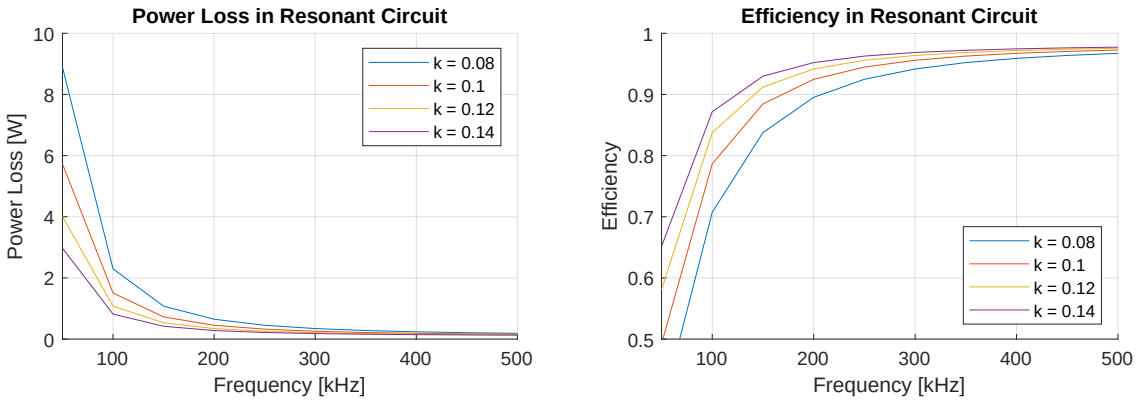

Figure 3.9: Power loss and efficiency of the resonant circuit (1)

Calculations with these formulas can be found in Section A.1.1 in Appendix A.1.

3.1.9. COIL RESISTANCE INFLUENCES

Not only the amount of power transferred is dependent on the frequency, but increasing the frequency also leads to an increase in the resistance of the coils as described in Section 3.1.5. Finding an optimum between these two is the next step of the analysis. The series resistance of the resonant circuit can be derived from Equation 3.12 and Equation 3.14:

$$R_{series} = \frac{\omega \cdot L}{Q} + \frac{DF}{\omega \cdot C} \quad [\Omega] \tag{3.24}$$

Replacing the equivalent series resistance of Equation 3.22 will lead to the following equation:

$$P_{loss} = P_{loss-1} + P_{loss-2} = P \cdot \left(\frac{1}{R} + \frac{R}{(\omega M)^2} \right) \cdot \left(\frac{\omega \cdot L}{Q} + \frac{DF}{\omega \cdot C} \right) \quad [W] \tag{3.25}$$

L is the inductance of the coil used, the chosen coil has an inductance of $24\mu H$ [17]. Q is the quality factor of the coil used (Figure 3.5). DF is the dissipation factor of the tuning capacitor uses, which is 0.1% or 0.001.

C is the capacitance of the tuning capacitor, which has been chosen to satisfy Equation 3.11 for different frequencies. This yields Figure 3.10 for the total power lost in the resonant circuit and its efficiency.

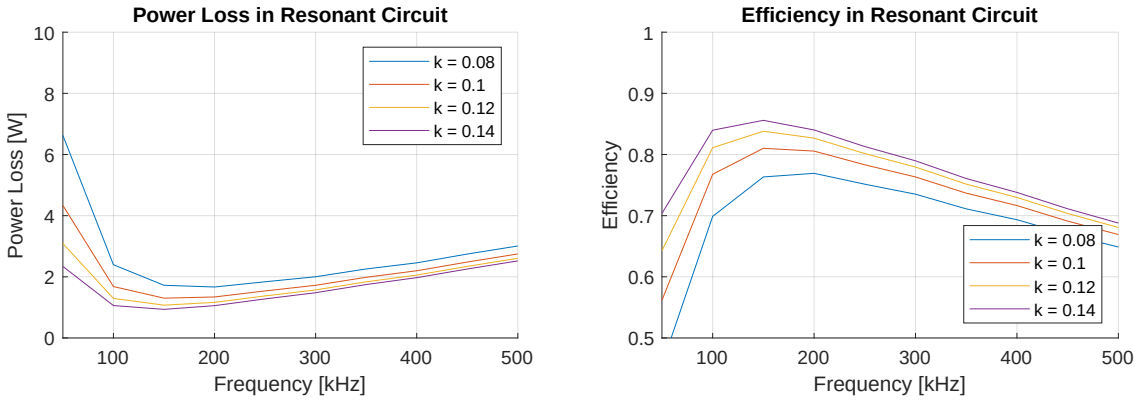

Figure 3.10: Power loss and efficiency of the resonant circuit (2)

Calculations with these formulas can be found in Section A.1.1 in Appendix A.1.
Using these figures, an operating frequency of 150kHz was chosen. At this frequency, the coil has an inductance of 25.3μH and a Q factor of 235. With formula 3.11, it can be calculated that with the resonance frequency at 150000kHz, the value of the tuning capacitor needs to be 44.5nF. Using formula 3.24 and the fact that the dissipation factor (DF) of the capacitor is 0.001, an equivalent series resistance of 125.3mΩ is calculated.

3.2. RECTIFIER

The receiving coil will deliver an AC signal at the resonance frequency determined by the combination of the values of the coil and the tuning capacitor. One of the requirements of the system is that the output has to be a DC signal. Because of this, an AC/DC converter will be necessary in the form of a rectifier. A rectifier uses diodes to let the current flow in one direction only, and a smoothing capacitor parallel to the load in order to approach a smooth DC signal. It is very important that the efficiency of this rectifier is as large as possible, since a 5W output power has to be reached at a receiver input power of just over 5W.

3.2.1. RECTIFIER REQUIREMENTS

The rectifier has to meet the following requirements:

1. A DC output voltage with a ripple of 2% at most.
2. The power transfer efficiency has to be as high as possible.
3. The rectifier has to be able to handle up to 2A and 20V (safe assumption).

3.2.2. RECTIFIER DESIGN CHOICES

A number of things had to be considered in order to design an ideal rectifier for the system requirements that were given. The most important requirement that the rectifier will influence is the total power efficiency. This is because the several components that will be used will dissipate a considerable amount of power, especially because according to equation 3.26 the relatively large average current value of 1A will flow through the rectifier circuit.

$$P_{average} = P_{out}/V_{out} = 5W/5V = 1A \tag{3.26}$$

Because of this the main goal of the design is to achieve an as large as possible efficiency.

FULL-BRIDGE VS. HALF-BRIDGE

The first thing that has to be considered when designing a rectifier is its configuration. The options are: half-bridge, regular full-bridge and a full-bridge with a center tap. Because the coils that were used do not have

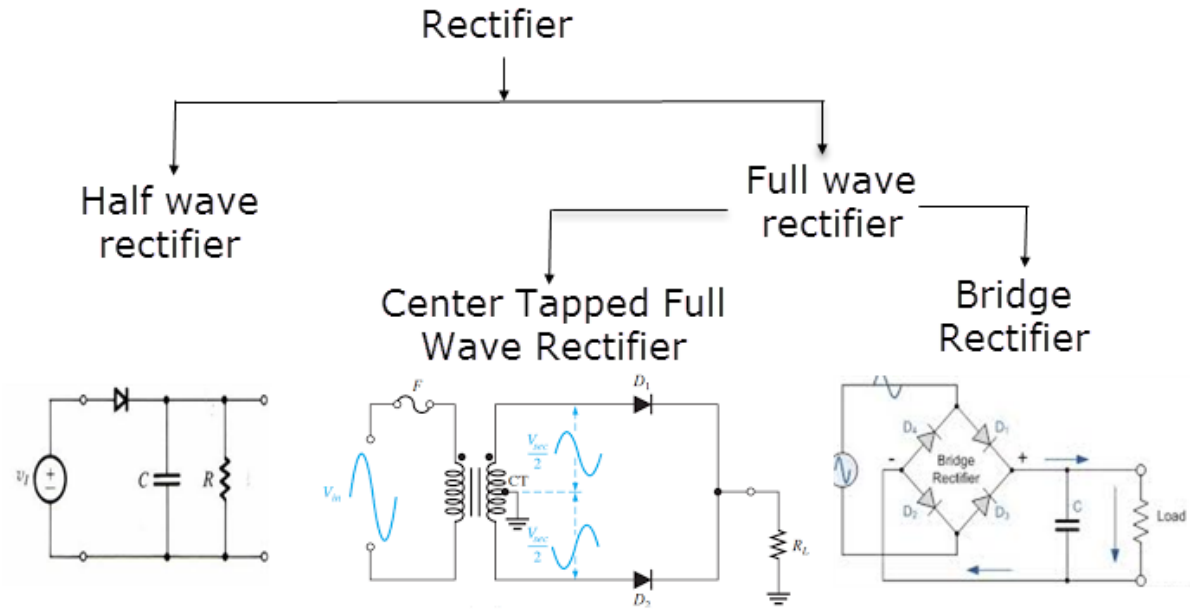

Figure 3.11: Types of rectifiers [21]

center taps, the last configuration is not an option. The main difference between a half-bridge and full-bridge rectifier is that a half-bridge rectifier will just use the positive voltage peaks for rectification, while a full-bridge

rectifier will use the positive as well as the negative peaks. The current through a full-bridge rectifier is shown in figure 3.13. It can be seen that no matter what side of the input source the current flows from, the current

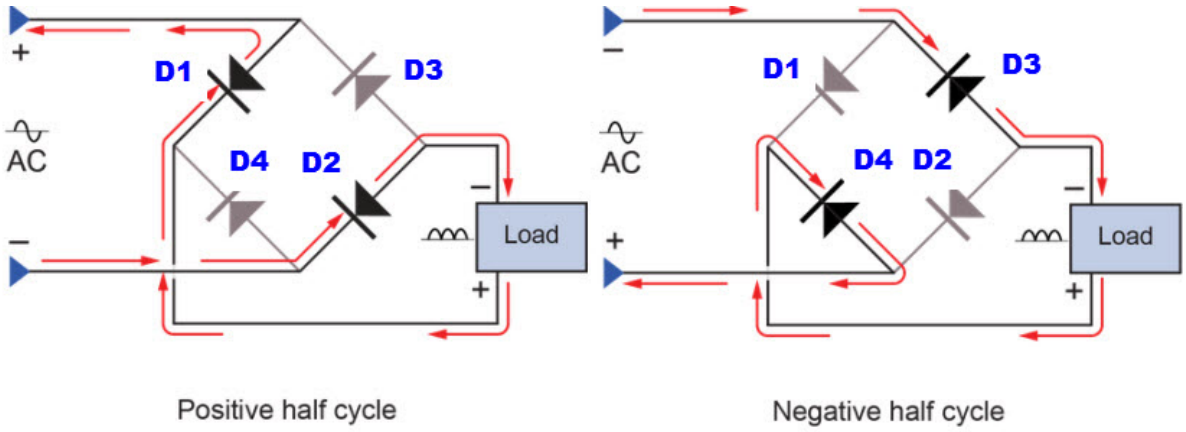

Figure 3.12: Current through a half-bridge rectifier [22]

will always flow through the load in the same direction.
It follows that the smoothing capacitor parallel to the load has to be larger for a half-bridge rectifier, since the voltage peaks are farther apart. Because of this, the capacitor will have to deliver energy for a longer time, which means that the capacitor will have to be able to store more energy.
Another effect is that the current peaks, and therefore the average current, flowing through the half-bridge rectifier will be twice as large as the current peaks through a full-bridge rectifier.

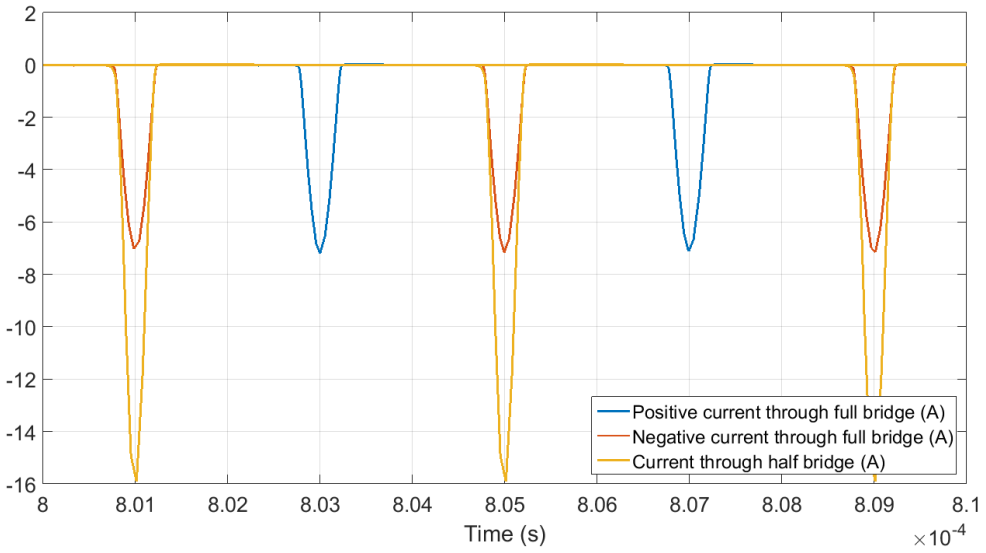

Figure 3.13: Current comparison full-bridge vs half-bridge

$$P_{diode} = V_{forward} * I_{average} \tag{3.27}$$

Formula 3.27 gives the power dissipation in a diode. From this formula it can be deduced that the power dissipated in a diode in a half-bridge rectifier will dissipate twice as much energy as a diode in a full-bridge rectifier diode. The current through a full-bridge rectifier however, flows through two diodes instead of one, so this effect is eliminated.

$$P_{full-bridge} = 2 * \frac{P_{half-bridge}}{2} = P_{half-bridge} \tag{3.28}$$

For resistive components however like wire/capacitor resistance or possible MOSFET on-resistance, the for-

mula for power dissipation is the following:

$$P = I^2 * R \tag{3.29}$$

Using formula 3.29 the formula for comparing the power dissipation in resistive components between a full- and a half-bridge rectifier becomes:

$$P_{full-bridge} = I^2_{fullbridge} R = 2 * (\frac{I_{halfbridge}}{2})^2 R = \frac{I^2_{halfbridge} R}{2} = \frac{P_{halfbridge}}{2} \tag{3.30}$$

So resistive components in a half-bridge will dissipate twice as much energy as they will in a full-bridge configuration. This effect was simulated and it was found that the RMS current in a half-bridge was around 1.4 times as large as in a full-bridge, which is still significant. Because of this and the fact that a full-bridge rectifier can function with a smaller smoothing capacitor, the full-bridge setup was chosen.

RECTIFYING COMPOMENTS

Another design choice had to be made for what kind of component to use to make sure the current only flows in one direction. The standard choice is regular diodes, but since these have a relatively large voltage drop of 0.7V on average, and an average current of around 1A will likely be flowing through them, P=V*I=0.7*1=700mW would be dissipated per diode, which is an undesirable amount compared to the 5W output. Especially considering that two diodes will dissipate this amount of power constantly.
A substitute for normal diodes is shottky diodes. These can have a voltage drop as low as 0.3V, which means they dissipate less than half the energy normal diodes dissipate. shottky diodes also have a faster recovery time, which means that they can be used for higher frequency applications, which is very favorable for this rectifier, since it will operate at a frequency of 150kHz. For this reason shottky diodes are preferred over normal diodes. The main drawback of shottky diodes is that they have a larger reverse current, meaning that they can handle a smaller reverse voltage before breaking down. But since they will not have to deal with voltages larger than 20V, this is not a problem.
A third option was using MOSFET transistors in order to rectify the current. For this to work, the gate signals of the MOSFETs must turn the MOSFETs on and off at the appropriate times. If this is not done properly, the current through the MOSFET will flow in both directions, and the current will not be rectified. The main advantage of using a MOSFET instead of a (shottky) diode is that they do not have a voltage drop, but a gate voltage-dependent ON-resistance, which can be as low as $10m\Omega$. As can be seen in figure 3.14, At lower

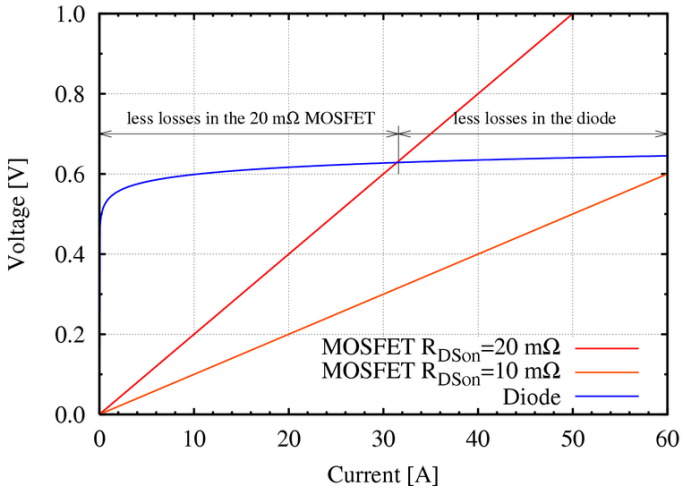

Figure 3.14: Voltage drop over a diode vs. a MOSFET [23]

currents MOSFETs will have significantly lower power dissipation through conductance than diodes (even shottky diodes as long as the voltage stays below 0.3V). Something to consider is that MOSFETs also have gate charge losses, which occurs because the charge stored in the gate is discharged, meaning the energy of this charge is lost. Because the gate discharges every period of the input voltage the following formula can be derived:

$$P = I * V = V_{GS} * \frac{Q_{gate}}{T} = V_{GS} * Q_{gate} * f \tag{3.31}$$

The last form of power loss that can occur in a MOSFET are body diode losses. MOSFETs have a diode connected in parallel, through which the current will flow if the MOSFET is not turned on properly. An example of this happening is when a high side and a low side MOSFET are both turned on for a short time. A lot of current will flow in this situation, so the body diodes will take over., This is an unwanted effect, since a relatively large amount of power will be dissipated in this diode. The following formula gives the power dissipation in the body diode of a MOSFET: [24]

$$P_{bodydiode} = V_{Fdiode} * I_{out} * t_{delay} * f \tag{3.32}$$

In this formula V_{Fdiode} is the forward voltage of the diode and t_{delay} is the amount of time for which both the high- and low side MOSFET are turned on (this is generally caused by switching delays). It follows that the total losses of a MOSFET are the sum of the conductive losses in formula 3.29, the body diode losses in formula 3.32 and the gate losses in formula 3.31. When choosing a MOSFET over a (shottky) diode, one needs to make sure that the sum of these losses are lower than than of the diode.

FINAL CONFIGURATION

Since MOSFETs have a significantly lower power loss than diodes if one with good specifications is chosen, it would be ideal to replace every diode in the rectifier with MOSFETs, meaning that the rectifier would contain 4 transistors. A number of attempts were made at achieving this.
The main difficulty of designing a diode-less rectifier is that the MOSFETs have to be turned on for the exact right amount of time at the exact right moment. Figure 3.15 shows the current through the diodes of a regular

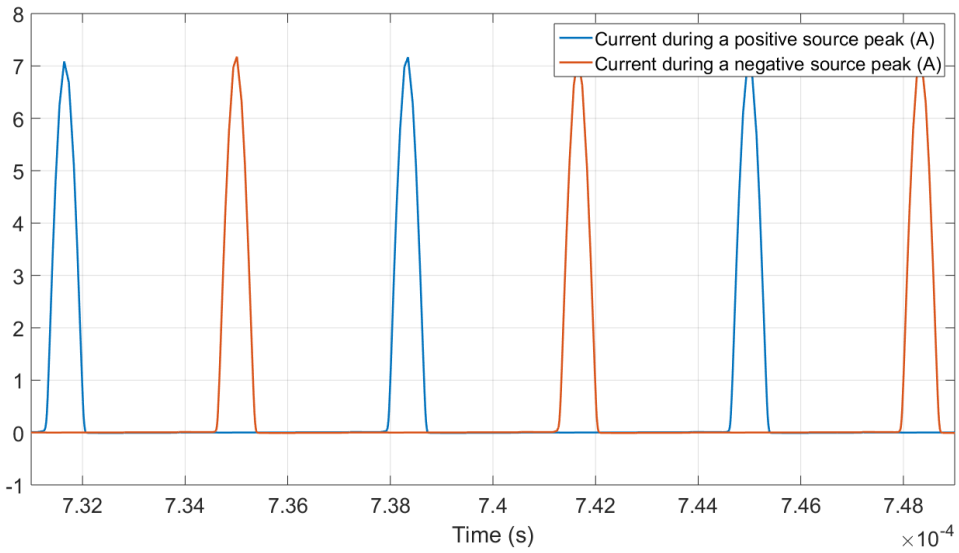

Figure 3.15: Current through the diodes in a regular rectifier in steady state ($V_s = 5.5V, 150kHz; R_L = 5\Omega$; C=500μF)

diode rectifier. It can be seen that the current flows through the diode in pulses, only at the moments where the source voltage is higher than the capacitor voltage. This only happens at the positive and negative peaks of the source voltage. This means that when using MOSFETs, the gates need a voltage pulse at the peaks of the source voltage. The main difficulty is that if the given pulse is too short, the capacitor will not be fully charged, meaning that the load will not absorb the highest possible power. Though if the given pulse is too long, the current will flow from the capacitor through the MOSFET in the direction of the source, since the MOSFET will still be open while the capacitor voltage has become higher than the source voltage. This will cause considerable losses.
The first attempt at a diode-less rectifier made the gate signals by comparing the AC coil voltage to a DC voltage slightly lower than the amplitude of the coil voltage. The result of this is shown in figure 3.16. The created pulses occur during the peak of the input voltage, which is the desired result. The length of the pulses can be determined by adjusting the reference voltage. If one would want shorter pulses, one would have to make sure the reference voltage is closer to the peak value of the coil voltage. Two comparators would be necessary in order to create pulses at both the positive and negative peaks of the coil voltage. The positive and

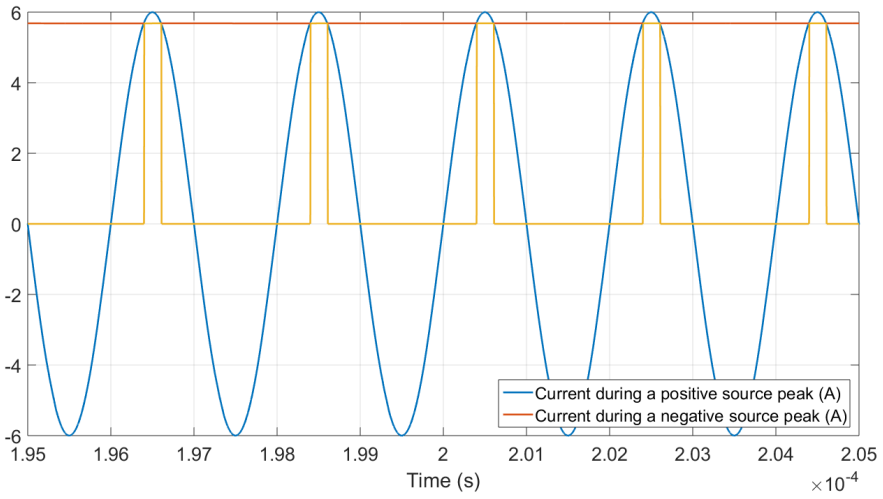

Figure 3.16: Plot showing how timed pulses can be produced using a comparator

negative supply voltages of the comparators could be created using two simple half-bridge rectifiers creating a positive and a negative DC voltage.
Since gates could only be directly driven by a push-pull comparator, which are generally slow, and since the gate voltage of the high side of the comparators would need to be higher than their supply voltage, a high side gate driver is needed between the comparator and the gates. Another advantage of using gate drivers is that they can deliver high current surges, which are necessary to quickly supply the gate charge necessary in the gate of a MOSFET since:

$$Q = I * t \tag{3.33}$$

This gate driver gives a lower voltage output for the MOSFET with the ground as its source, and a higher voltage output for the MOSFET with its source connected to the +-side of the load. Two gate drivers would be needed in order to make sure that only two of the four MOSFETs are turned on at all times. The created gate signals would be 180° out of phase. The proposed circuit is shown in figure 3.17. In this circuit, the current

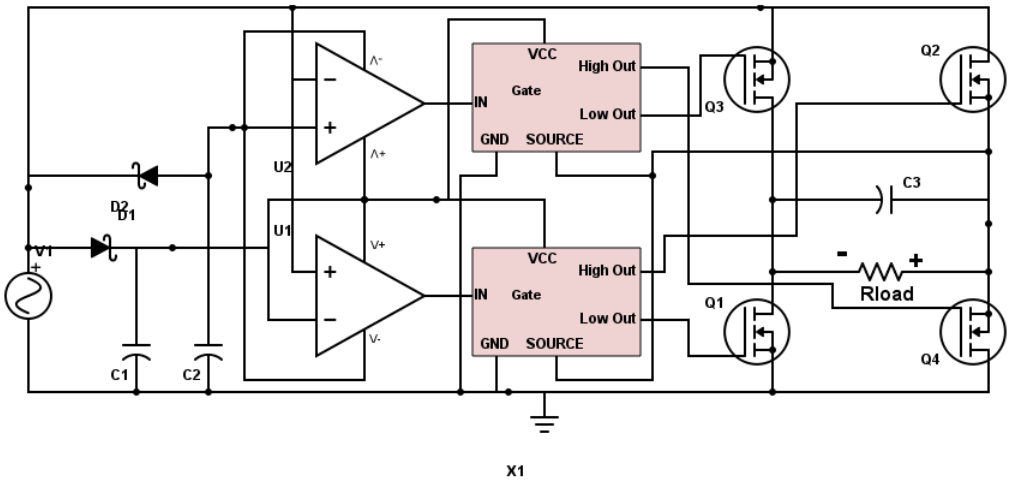

Figure 3.17: Full schematic of an attempted diodeless rectifier

will flow from the top-right to the bottom-left MOSFET when the source voltage is negative, and from the bottom-right to the top left MOSFET when the source voltage is negative.
The first problem with this design is that, because of the voltage drop over the two rectifying diodes at the start of the circuit, the reference voltage could not be large enough in order to get the produced pulses short

enough. This means that the MOSFETs are turned on for a too large period, causing the current to flow in the wrong directions as shown in figure 3.18 It would be possible to fix this problem by enlarging the reference

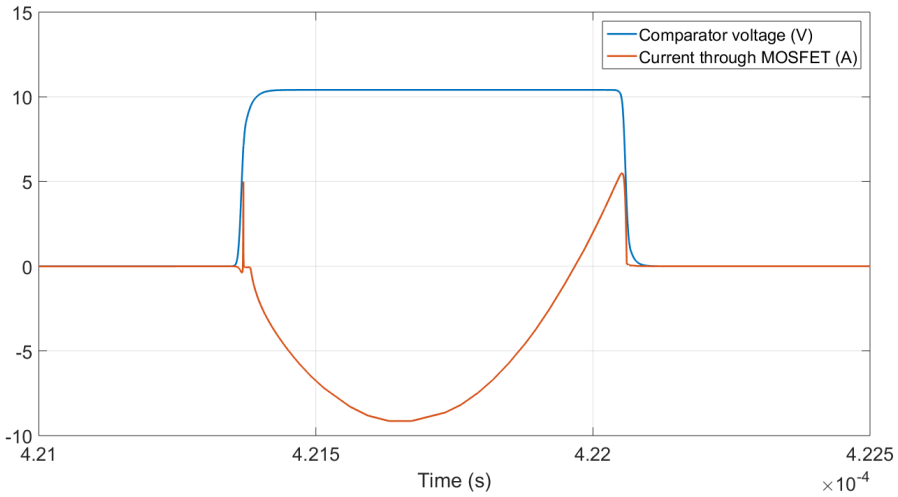

Figure 3.18: A figure showing the current through a MOSFET in schematic 3.17

voltage somehow, but the biggest problem will remain: The length of the pulses is dependent on the voltage over the diodes, the amplitude of the AC input voltage and the stability of the input voltage. The reference voltage would have to be the perfect amount at all times, or the system would become highly inefficient. For this reason this circuit was not used in the final implementation of the rectifier.
After this another implementation was tried. This made use of the idea that current should only flow through the MOSFETs when the coil voltage is higher than the voltage over the load. If a comparator is used to compare the coil voltage to the load voltage, perfectly timed and sized pulses should be created which would drive the MOSFET gates so that the current will only flow in the desired direction. This implementation can be seen in figure 3.19. The problem with this design is that the comparators do not correctly detect when current

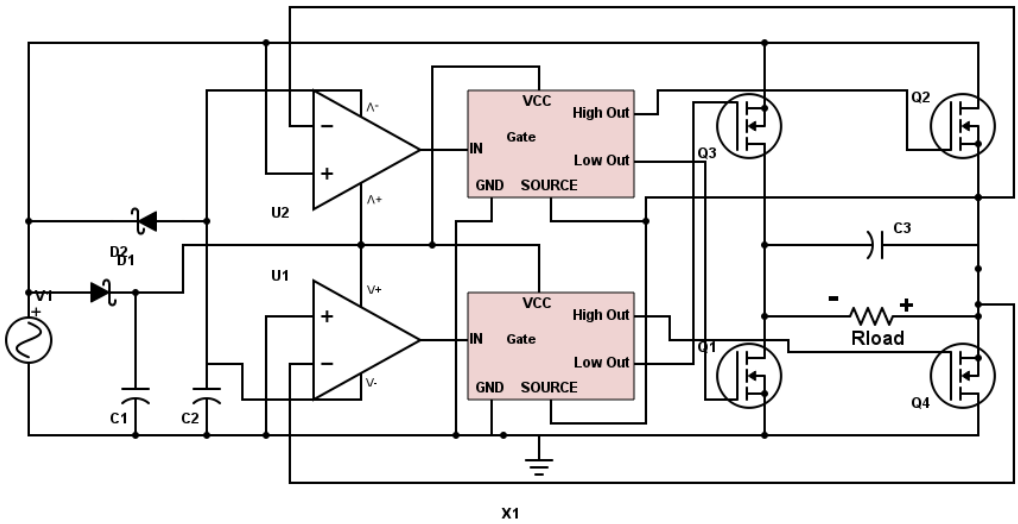

Figure 3.19: Full schematic of an attempted diodeless rectifier

needs to flow. In the simulation of the circuit, it was observed that the comparators only gave pulses every three or four periods, causing the power transfer to the load to be minimal, as can be seen in figure 3.20. Because of complexity, unreliability and time constraint, it was decided that a full MOSFET rectifier would not be implemented.

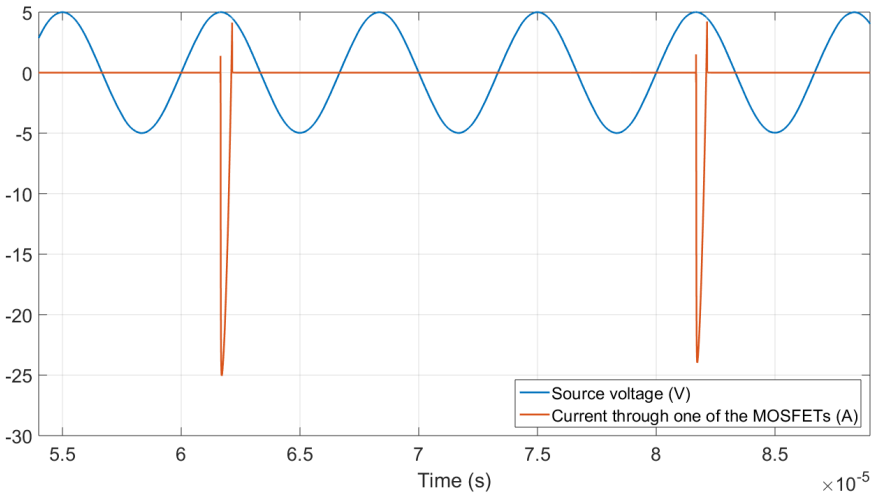

Figure 3.20: A figure showing the current through a MOSFET in schematic 3.19

A simpler rectifier has been implemented that uses two shottky diodes and two MOSFETs. Because of the diodes, the current will not flow in the wrong direction, even if the MOSFETs are turned on for a relatively long time. The system is not as efficient as the diode-less rectifier would have been, but because two out of four diodes are replaced with MOSFETs, it is still more efficient than the standard full-bridge rectifier. The gates are driven by the opposite side of the coil. Because of the gate-source voltage of the MOSFETs will be the amplitude of the coil voltage at the time the current conducts (during the peaks of the coil voltage). The final rectifier design can be seen in figure 3.21. NMOS transistors were chosen over PMOS transistors, since NMOS

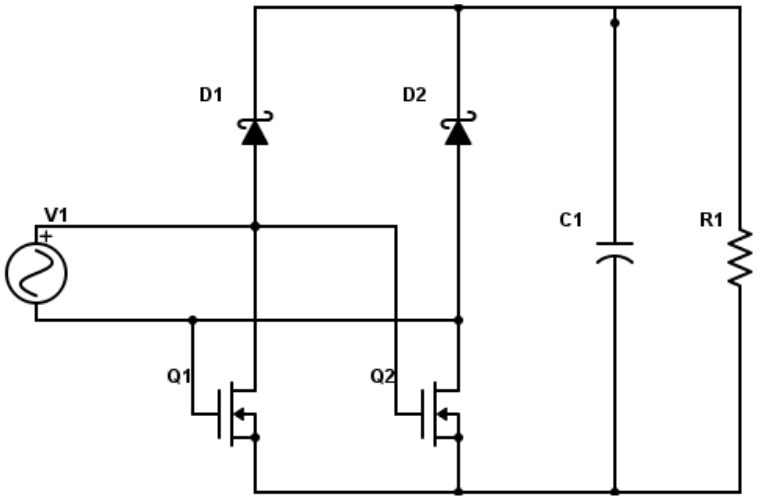

Figure 3.21: Full schematic of the implemented rectifier

generally have a lower on-resistance and/or gate charge. Body diode losses will not occur, since this design only has low-side MOSFETs. A high side gate driver could have been used to enlarge the gate-source voltages of the MOSFETs, which would lower the on-resistance of the MOSFETs. But some calculations have been done considering the difference in conductance loss, gate charge loss, and gate driver power consumption, which showed that this was not profitable. These calculations will be given later in this thesis.

COMPONENT SELECTION

In order to finalize a maximally efficient rectifier, the used components have to be selected so that they are ideal for the specifications. Another important thing to consider is that the components have to be able to

handle the currents and voltages as described in the requirements for the rectifier.
For the shottky diodes, the only aspect that influences the efficiency is its forward voltage. The selection of the used shottky diodes was done by searching for the diode that can handle at least 2A/20V with the lowest forward voltage, that the manufacturer (Farnell[25]) could deliver. With this process, the STPS20L25CT shottky diodes [26] were chosen. It can handle a repetitive voltage of 25V, an average forward current of 10A and has a low voltage drop of 300-350 mV. This means that with an average current of 1A (which is required for a system output of 5V/5W) both diodes combined will dissipate P=0.35*1=350mW, which is acceptable. This is a dual common cathode diode, and because the cathodes of the diodes in the setup are connected (to the positive side of the load) only one STPS20L25CT is needed.
Next, the NMOS had to be chosen. There are a number of things that have to be considered: the maximum gate-source voltage, the drain-source breakdown voltage and drain current should be high enough, the threshold voltage should not be too large, or the transistor will not be turned on correctly, and a good combination of low gate charge and low on-resistance has to be found. Rise and fall times are less important in this situation, since the MOSFETs will have been turned on some time before the current will flow as can be seen in figure 3.22, so no fast on and off switching is necessary. The threshold voltage of most MOSFETs is between 1V and 2V, and since the gate-source voltage will have the same value as the coil voltage, the thresh hold voltage will likely not be the most important factor. Low gate charge and low on-resistance is a trade off in MOSFETs. The best balance between the two for the specifications has to be found. The losses of a MOSFET (that has no body diode losses) is given in formula 3.35 [24].

$$P_{dissipated} = I^2 * R_{on} + Q_{gate} * V_{GS} * f \tag{3.34}$$

In order to select the optimal transistor, the RMS current through the transistors needed to be known. The formula to calculate the RMS value for a signal is given below.

$$I_{RMS} = \sqrt{\frac{1}{T_1 - T_2} \int_{T_1}^{T_2} (I(t))^2 dt} \tag{3.35}$$

I(t) being the current signal over time. The circuit was simulated in LTspice in order to see the behaviour of the MOSFET current. The results of this simulation can be seen in figure 3.22. A source voltage of 5.5V was

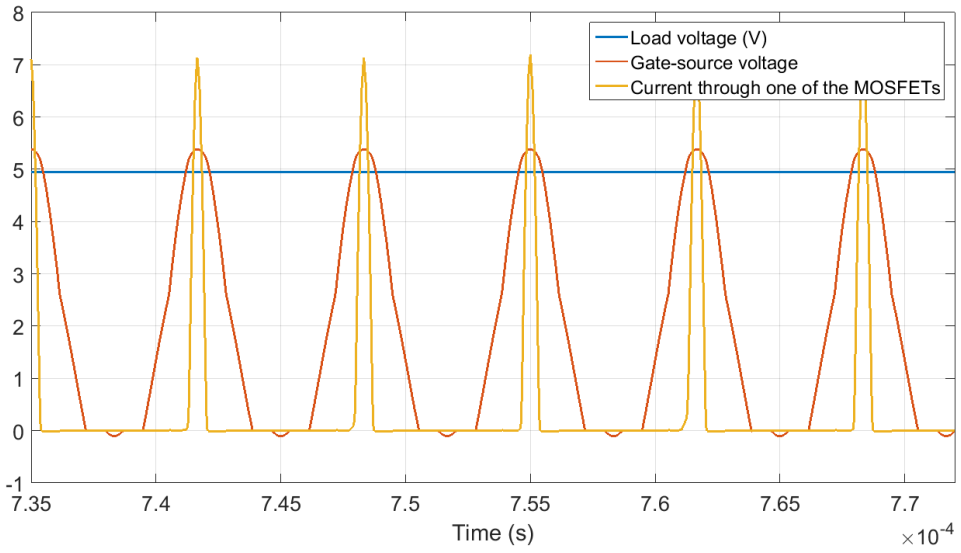

Figure 3.22: Simulation of the MOSFET current (V_{source} : 5.5V, 150kHz; R_{load} : 5Ω;C=500μF)

chosen so that the voltage over the load would be 5V (voltage drop of approximately 0.5V), so that with a load resistance of 5Ω a 5W/5V output is achieved. The current has triangular shaped peaks when the coil voltage surpasses the load voltage (or when the coil voltage drops under 0V for the other MOSFET). The calculation for the current signal is non-linear and difficult to do by hand, so LTspice's calculated RMS current of the signal will be used. LTspice gave an RMS value for the steady state current of 1.624A.

The chosen transistor is the Si4128DY [27]. It can handle a drain-source voltage of 30V, a gate-source voltage of 20V and 10A drain current. At 4.5V it has a gate capacitance of 3.8nF and an on-resistance of 24mΩ. If a current of 1.624A, a gate-source voltage of 5.5V and a frequency of 150 kHz are used, formula 3.35 gives a power dissipation of 66.4 mW per MOSFET. This gives a total MOSFET dissipation of around 133 mW, which is significantly less than the 350 mW of the diodes. Attaching a high side gate driver to the MOSFET gates could possibly have lowered the total power dissipation. If the gate voltage would have been driven up to 10V, the datasheet [27] tells that the on-resistance would become 20mΩ and the total gate capacitance would become 8nF. From formula 3.35 a power dissipation of 64,7mW per MOSFET can be calculated. The difference in power would be 66.4-64.6=1.8mW, since a typical high speed, high side gate driver like the UCC27714 by Texas Instruments [28] uses up to a few mW, it was decided that it is not profitable to implement gate drivers in the rectifier.
Normally a value for the smoothing capacitor has to be decided, but as mentioned later in this thesis, the final design of the receiver lets the necessary value for the capacitor be dependent on factors that are not dependent on the rectifier. The capacitor selection will be mentioned later.
Further in this thesis will be shown that the smoothing capacitor losses are minimal, but a prediction can be made of the power efficiency of the system. This can be calculated with the following formula:

$$\eta = \frac{P_{output}}{P_{output} + P_{diodes} + P_{MOSFETs}} \tag{3.36}$$

Inserting the calculated values into formula 3.36 gives an efficiency of 91.2%.

3.2.3. SIMULATIONS

Figure 3.21 was simulated in LTspice with SL43 shottky diodes and IRFHS8284PbF MOSFETs, since the no LTspice models for the selected components were available. The specifications of the simulated components are comparable to those of the selected components. The ground was placed at the negative side of the load. The voltage source delivers 5.5V at 150kHz, the capacitor value was 500 μF (safe value since the capacitor size has not been decided yet) and the load was 5Ω. Figure 3.23 shows the simulated input and output of the rectifier. The figure shows that the voltage is properly rectified and that the total voltage drop is around 0.5V,

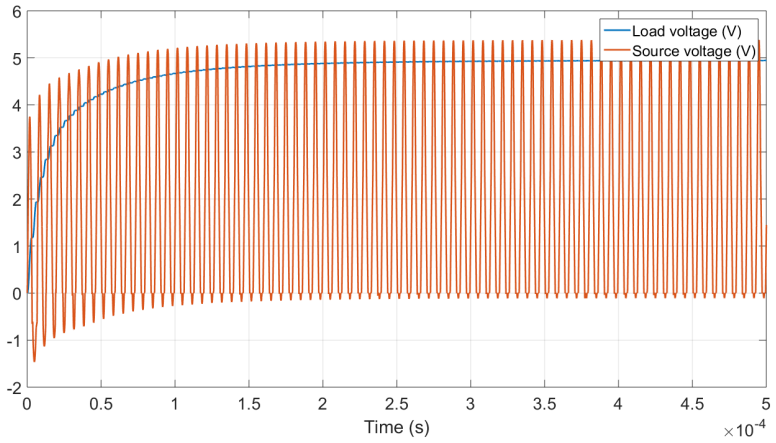

Figure 3.23: The simulated input and output of the rectifier circuit

which is acceptable.
The average power delivered by the source in steady state is 5.3076W and the average power delivered in the load is 4.8785W. This gives an efficiency of 92.6%, which is very close to the earlier calculated efficiency. If a schematic with the same source and load is simulated using only shottky diodes to rectify the current an efficiency of 86.7% is simulated. The same schematic with the shottky diodes replaced by normal diodes gives an efficiency of 66.5%. Figure 3.17 gives an efficiency of 88.6%, but it needs a very high input voltage in order to deliver 5W to the load. Figure 3.19 shows an efficiency of 90.7%. It is clear that the schematic in figure 3.21 is the most efficient configuration.

3.3. DC-DC CONVERTER

3.3.1. DC-DC CONVERTER REQUIREMENTS

The DC-DC converter has to meet the following requirements:

1. The converter has to convert the DC input signal into a 5V/5W output signal.
2. The output voltage ripple can not be larger than 2%.
3. The power loss should be as low as possible.
4. The circuit has to be designed in a way so that it is compatible with the rectifier and the resonant circuit.

3.3.2. DESIGN CHOICES

An output power of around 5W is required, this can be obtained by putting 5V over a 5Ω load resistance. The output voltage is known, so the input voltage will determine which DC-DC converter will be implemented. Linear voltage regulation dissipates the unwanted power as heat. These losses are unacceptable due to the strict efficiency requirements. Switching conversion seems to be a better solution, as it is more power efficient. Step-down Buck switching converters are mostly more efficient, but step-up boost switching converters are sometimes unavoidable. The DC-DC converter is the last component before the load and therefore depends on the rest of the system. The expected input parameters were predicted while making the first design choices of the DC-DC converter. More than one possible solution were hence suggested and implemented in the complete system in a later stage.

3.3.3. IMPLEMENTATION

Multiple buck-boost converter chips with adjustable in- and outputs are available on the market, some even with a variable input and a fixed 5V 1A output.

ADP2504-5.0

The ADP2504-5.0 [29] is a high efficiency buck-boost converter that can operate with input voltages between 2.3V and 5.5V, it has an output voltage of 5.0V and a output current of 1000mA. Single device tests as is shown in figure 3.24a resulted a steady 5W output in the range of 4-5.5V input, which seemed the right range for this system, because rectifier output voltages lower than 5V were measured during the first system simulations.

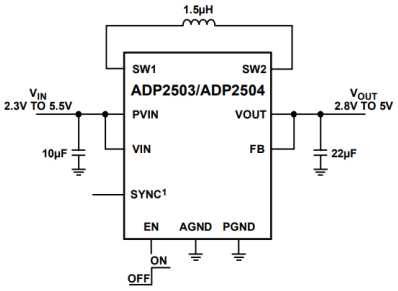

(a) Test circuit of the ADP2504-5.0 [29]

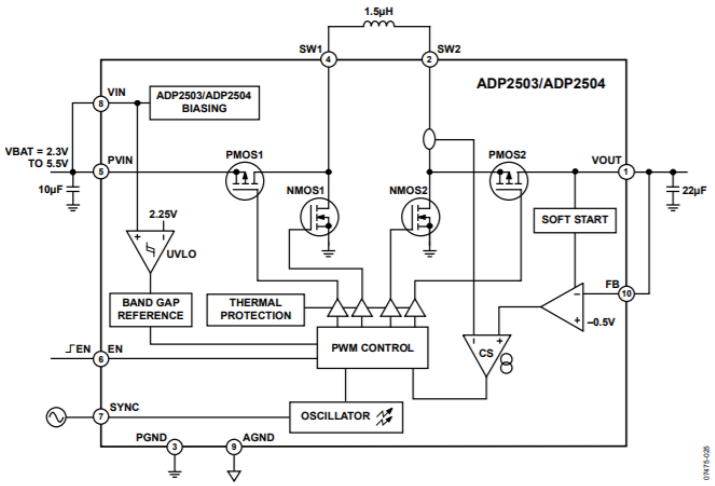

(b) Internal block diagram of the ADP2504-5.0 [29]

Figure 3.24b shows us an internal block diagram of the ADP2504-5.0. 4 Four internal MOSFETs are controlled by a PWM controller, these four MOSFETs determine the rate of charge and discharge of the external inductor between SW1 and SW2 [29]. Three different modes can be distinguished: Buck, Boost and Buck-Boost. PMOS2 is always active, NMOS2 is always off and PMOS1-and NMOS1 are both switching in antiphase to maintain a constant output in Buck mode. For boost operation the exact opposite happens: PMOS1 is always active, NMOS1 is always off and PMOS2-and NMOS2 are both switching in anti-phase. Both operations

combined results in the two MOSFETs on the left side are in anti-phase and the same accounts for the two on the right side. The MOSFETs switch with a frequency of 2.5MHz for a minimal output ripple and to minimize the size of the external inductor. Output voltage can be controlled with a voltage divider between V_{out} and FB (R1) and between FB and GND (R2):

$$V_{out} = (\frac{R1 + R2}{R2}) * V_{ref} \tag{3.37}$$

The results from implementing the ADP2504-5.0 were unfortunately not as expected. The maximum input voltage almost directly exceeded the 5.5V limit. This happens because the output of the converter is a constant power, meaning that the input of the converter will also have a constant power. From formula 3.38 it follows that if the input voltage of the buck/boost converter rises, the current will become smaller.

$$P = V * i \tag{3.38}$$

Formula 3.39 shows that the input resistance of the buck boost converter will then increase when the input voltage increases.

$$R_{in} = \frac{V_{in}}{I_{in}} \tag{3.39}$$

When the load resistance of the receiver increases, more power will be transmitted, meaning that the input voltage will increase (the proof for this will be given later in this section). Fro this it follows that once 5V/5W output is reached, the input voltage of the buck/boost converter will increase, after which more power is transferred by the transmitter, after which the input voltage will increase even further. A positive feedback loop exists that will make the input voltage of the converter rise to a very large value.

Even tough the device kept working in ltspice, it probably will break down when implemented in the system. The internal components in combination with the external inductor are not suited to step-down from such high voltages. The input voltage reached a maximum at 25V as shown in figure 3.25. This is likely because the used LTspice model for the converter allows a maximum input voltage of 25V.

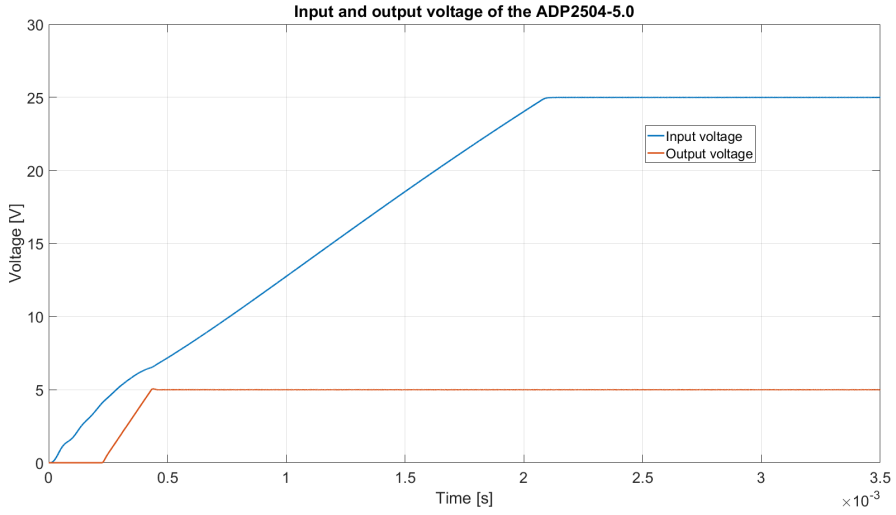

Figure 3.25: Input and output voltage of the ADP2504-5.0

LTC3114-1.0

The LTC3114-1 [30] is a wide operating voltage range synchronous buck-boost converter that can operate with input voltages between 2.2V and 40V. It has a wide output range of 2.7V up till 40V with an output current of 1A in buck mode. Test with this single device as figure 3.26a showed that a fixed 5V 1A output can be generated with inputs from 6V.

This Buck-Boost converter works by the same principle as the one mentioned in 3.3.3. The inductor between SW1 and SW2 in figure 3.26a will be charged and discharged by different switching rates of the internal

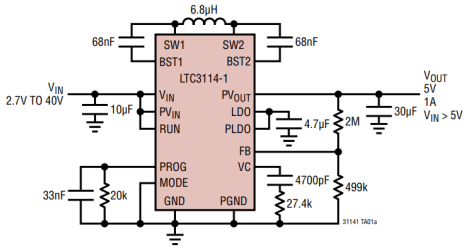

(a) Test circuit of the LTC3114-1.0 [30]

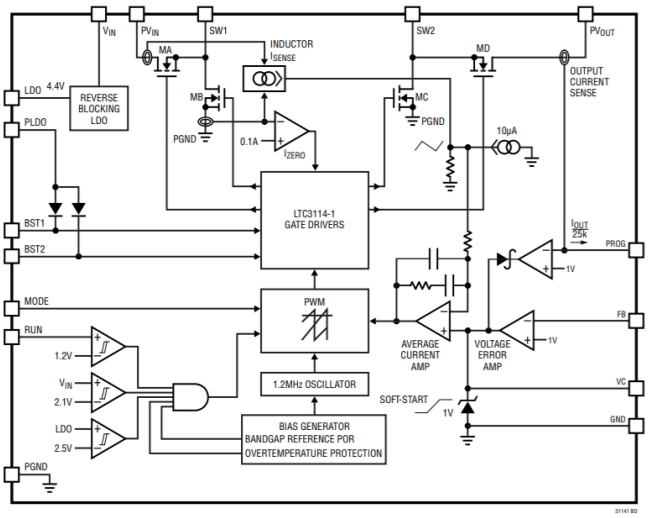

(b) Internal block diagram of the LTC3114-1.0 [30]

MOSFETs of figure 3.26b. The gate driver of the MOSFETs is controlled by a 1.2MHz PWM signal [30]. Two flying capacitors from SW1 to BST1 and from SW2 to BST2 are there to generate the gate driver rail for power switch A and D respectively.

The input voltage of the buck-boost converter again raises up until 25V as can be seen in figure 3.27. In reality this voltage will rise to larger values, causing also this chip to break down.

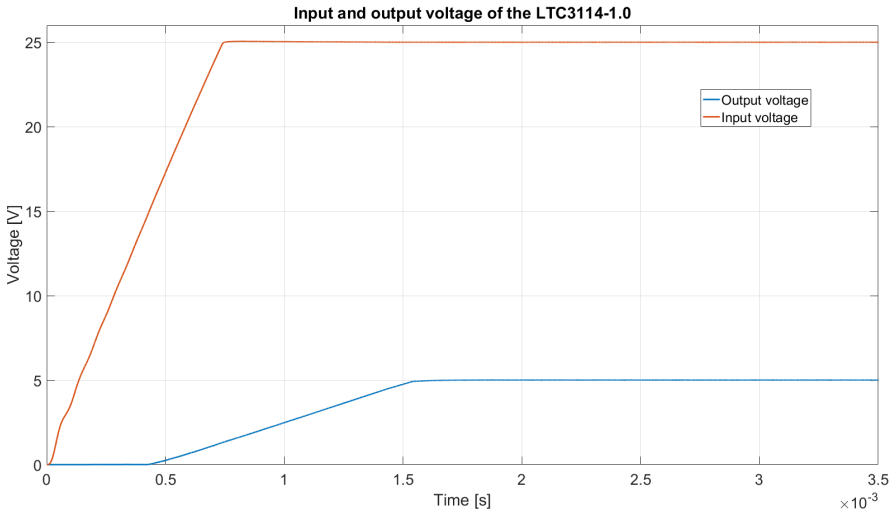

Figure 3.27: Input and output voltage of the LTC3114-1.0

Apart from the high voltages, the simulated efficiency of the receiver containing the resonant coupled coils, the rectifier and one of the buck/boost converters were very poor: mostly less than 50%. This inefficiency grew worse as the transmitter voltage increases. This is because after the load voltage has reached 5V, the receiver needs less power to maintain this voltage. Because of this a power surplus is created. A way needed to be found in order to regulate the power that is transmitted.

VOLTAGE REGULATOR

Unfortunately it was not possible to meet the requirements with the previous two solutions, so other options without buck-boost converter chips needed to be considered. The 'around' 5W output requirement gave some room to implement a DC-DC converter with a small output ripple. A voltage regulator, as shown in figure 3.29, makes this happen.

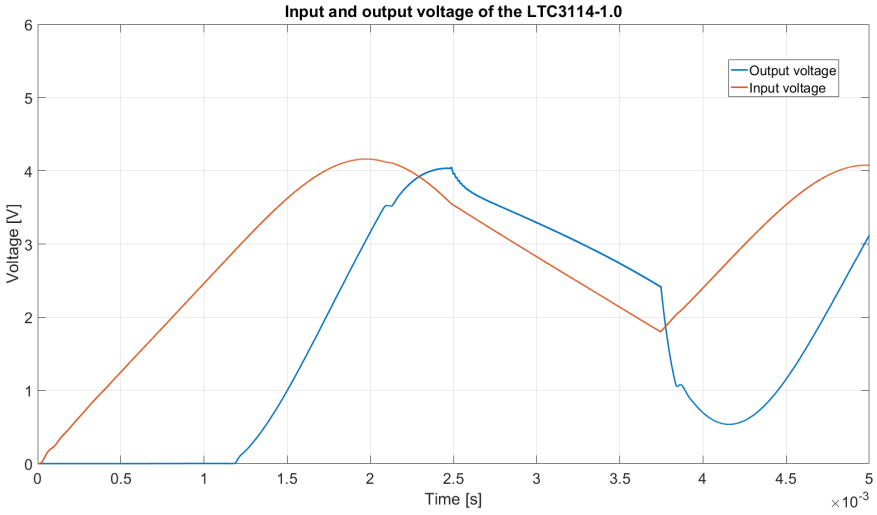

Figure 3.28: Input and output voltage of the LTC3114-1.0

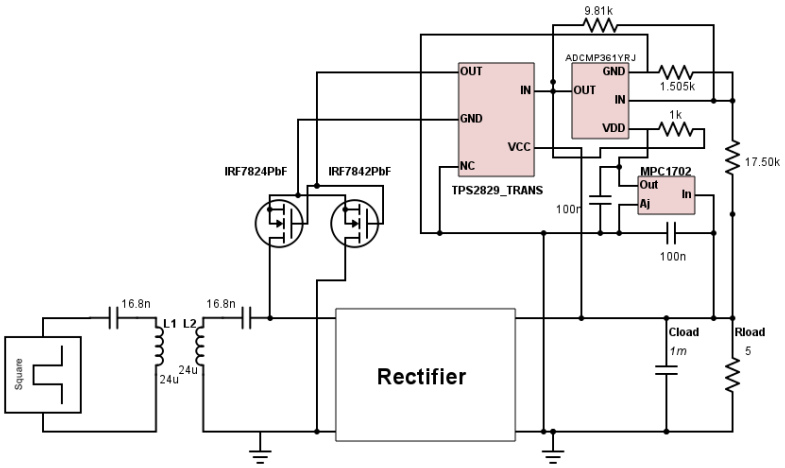

Figure 3.29: Voltage regulator schematic

The idea behind this voltage regulator is that the resonant circuit is only connected to the load if the smoothing capacitor after the rectifier is not able to deliver enough power anymore. At any other moment a short circuit will be created after the resonant circuit. The rectifier will charge the load capacitor until the voltage over the load resistance rises above 5V. The 400mV reference comparator and the gate driver both have a low output voltage during that time. The comparator is activated when the voltage over the load resistance becomes larger than 5V and therefore the input voltage of the comparator becomes larger than 400mV as a result of the voltage divider relative to the ground.

$$V_{in} = \frac{1.505k}{1.505k + 17.5k} * 5V = 396mV \approx 400mV \tag{3.40}$$

The comparator is supplied by the output voltage of the rectifier and has an internal reference voltage of 400mV. Once the input voltage of the comparator becomes larger than 400mV, its output signal will be high, turning the gate driver on. This gate driver is necessary because otherwise, a push-pull comparator is needed to properly drive MOSFETs gates, and push-pull comparators are generally not quick enough. The gate driver will immediately turn on the coil-shorting MOSFETs. This causes the load capacitor to discharge and deliver power to the load resistance until the voltage over the load resistance drops below 5V. The input voltage of the comparator will then become smaller than 400mV and the comparator output turns low again. The gate

driver will turn off, which causes the complete system to charge the load capacitor as before.
This means that the receiver has two modes: the rectifier mode and the short circuit mode. The schematic of these modes is shown in figures 3.30 and 3.31. The main difference between these modes is the resistance in

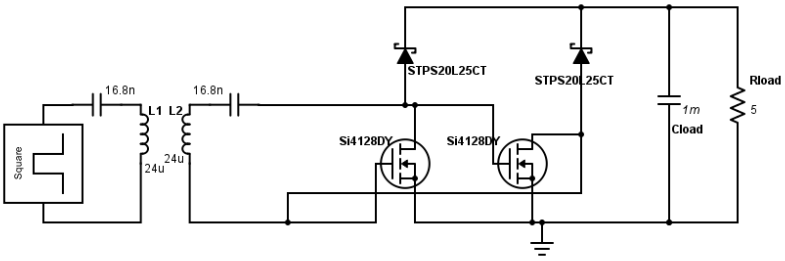

Figure 3.30: Rectifier mode

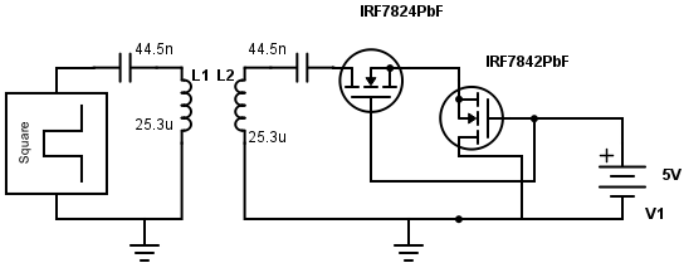

Figure 3.31: Short circuit mode

the circuit.

An equivalent circuit of the transmitter and receiver is shown in figure 3.32. E_M is the induced voltage created by the magnetic field through the receiving coil, it is added to the receiving side as a source and generates power for the load. Z_E on the transmitter side is the reflected impedance of the receiver.

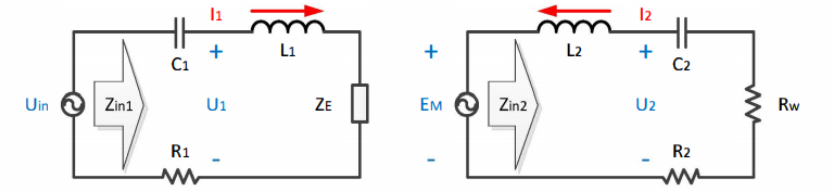

Figure 3.32: Decoupled equivalent circuit

The equivalent impedance seen from the source E_M can be determined with equation 3.41[20].

$$Z_{in2} = j\omega L_2 + \frac{1}{j\omega C_2} + R_2 + R_w = \frac{E_M}{-I_2} = \frac{j\omega M * I_1}{-I_2} \tag{3.41}$$

The reflected impedance is then given by:

$$Z_E = \frac{j\omega M * I_2}{I_1} = \frac{(j\omega M)^2}{Z_{in2}} \tag{3.42}$$

When the LC circuit is shorted by the two MOSFETs the input impedance of the receiver changes to:

$$Z_{in2} = j\omega L_2 + \frac{1}{j\omega C_2} + R_2 + 2 * R_d s \tag{3.43}$$

The equivalent working resistance R_W is a lot larger compared to the equivalent resistances of the coil and capacitor, so Z_{in2} is primary determined by R_W. As can be seen in figure 3.30 and 3.31, R_W switches between the resistance of the load, the rectifier MOSFETs and the diode resistance, to just the resistance of the shorting MOSFETs. Replacing R_W with combined R_{DS} resistances of the MOSFETs, which is small, results in a large decrease of Z_{in2}. From equation 3.42 can derived that Z_E becomes extremely large when the mutual inductance stays the same. Because the AC voltage in the transmitter stays the same and reflected impedance becomes very large, the current through the transmitter goes almost to zero. The power supply delivers less power to the transmitter during that time, which increases the overall efficiency of this WPT-system. It can be seen that with this solution the opposite happens from what happened with a buck boost converter: for a buck/boost converter, the (input)resistance grew as the voltage grew, causing a positive feedback loop, while with this solution, the resistance in the loop is greatly reduced, making sure there is a negative feedback loop. Because of this, this is a stable system.

FREQUENCY BEHAVIOUR

Another way to look at the behaviour of the voltage regulator, is in the frequency domain. Figure 3.30 and 3.31 were simulated in the frequency domain to show this. Figure 3.33 and 3.34 show the current, and thus the power, that the source delivers for different frequencies for both modes. In these plots it can be seen

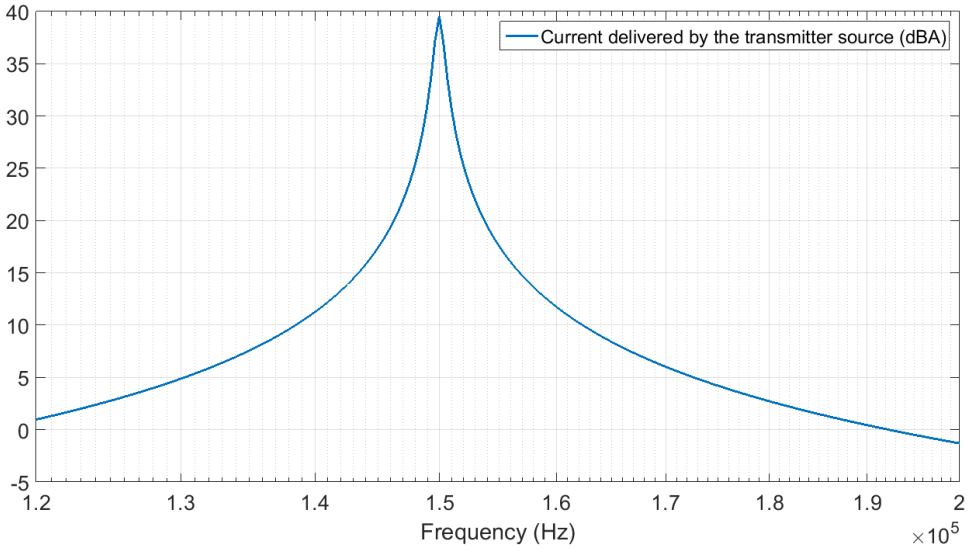

Figure 3.33: Frequency plot of the transmitter source current during rectifier mode

that the rectifier mode has a clear peak at 150kHz, while the short circuit mode had two peaks which are shifted to both sides of 150kHz, while at 150kHz a minimum can be observed. The frequency at which the transmitter makes the resonant circuits oscillate is set at 150 kHz, which means that for rectifier mode the transmitter current will be amplified, while in the short circuit mode the source current will be damped. This is the required effect, because during short circuit mode the receiver current (which will be the same as the transmitter current because the winding ratio is 1) has to be as low as possible, in order to minimize the losses. The two peaks in the short circuit simulation can be explained by the effect of frequency splitting. Frequency splitting is the phenomenon that the peak in a frequency domain of a resonant coupled circuit splits into two peaks which are shifted to the left and right of the original peak, when the coils are over coupled.

In figure 3.35 it can be seen that while the coils are under coupled, a single peak remains which becomes higher as the coupling increases. When the coils are over coupled, it can be seen that the peak splits, and that the peaks are shifted further as the coupling increases further. The border between these two areas is called the critical coupling coefficient. If the coupling surpasses the critical coupling coefficient, the frequency peaks will split. The formula for this coefficient is as follows. [32]

$$k_c = \frac{1}{\sqrt{Q_1 * Q_2}} \tag{3.44}$$

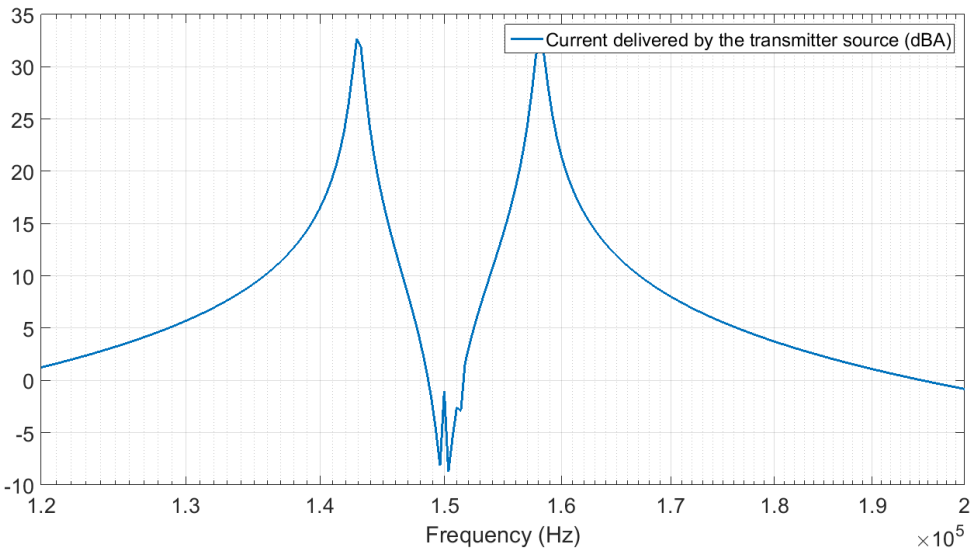

Figure 3.34: Frequency plot of the transmitter source current during short circuit mode mode

Q_1 will be the same for both modes, since nothing changes in the transmitter [1]. The value of Q_2 however, will change, because it is dependent on the resistance in the RLC loop, which is different for both modes. The Q factor of a series RLC circuit is the following:

$$Q = \frac{1}{R}\sqrt{\frac{L}{C}} \tag{3.45}$$

When the receiver is in short circuit mode (figure 3.31), its resistance in the current loop is far smaller than its resistance in rectifier mode (figure 3.30). Because of this, the Q factor will be much larger according to 3.45. From formula 3.44 it then follows that the critical coupling coefficient will be much lower, causing the frequency peaks to split at much lower coupling factors. This is observed in figure 3.33 and 3.34: at the same coupling factor, the frequency peak splits for short circuit mode, but it does not split for rectifier mode.

BUILT-IN REFERENCE COMPARATOR SELECTION

The comparator has to have a built-in reference that is achievable through a voltage division from 5V, needs to be quick and accurate enough, and its output needs to be able to turn a gate driver on and off. If the comparator is not accurate enough, the output signal could turn on too late or too early, causing the MOSFETs to turn on too late or too early, which would cause a larger ripple on the output. If the comparator's propagation delay is too small, the MOSFETs will turn on too late, having the same effect as the previously mentioned problem.
For this the ADCMP361YRJ comparator from Analog Devices [33] was chosen. It has a 400mV reference voltage with a threshold voltage accuracy of 0.275%. The maximum voltage ripple that could be caused by this inaccuracy is 2*0.275%=0.55%, which is a small enough amount if a maximum ripple of 2% may be achieved. The chip has a typical supply current of 7μA at 5.5V, which gives a power dissipation of 38.5μW, which is an insignificant amount compared to the output power. The ADCMP361YRJ has a response time of 5 μs and a rise time/fall time of around 0.3μs. The effect of delays in the voltage regulator can be seen in figure 3.36 In this figure it can be seen that the comparator's output turns on some time after the load voltage has surpassed the 5V threshold. During this time, the voltage will continue rising or falling with its initial slope. With the delay time and the current through the smoothing capacitor the voltage ripple caused by delays can be calculated. The RMS current through the capacitor is dependent on a lot of factors, but the later explained LTspice simulation shows that it is generally around 1.5A (combination of the RMS current while rising and falling) for a capacitor of 1mF. The formula 3.46 shows the current through a capacitor.

$$I_C = C\frac{dV_C}{dt} \tag{3.46}$$

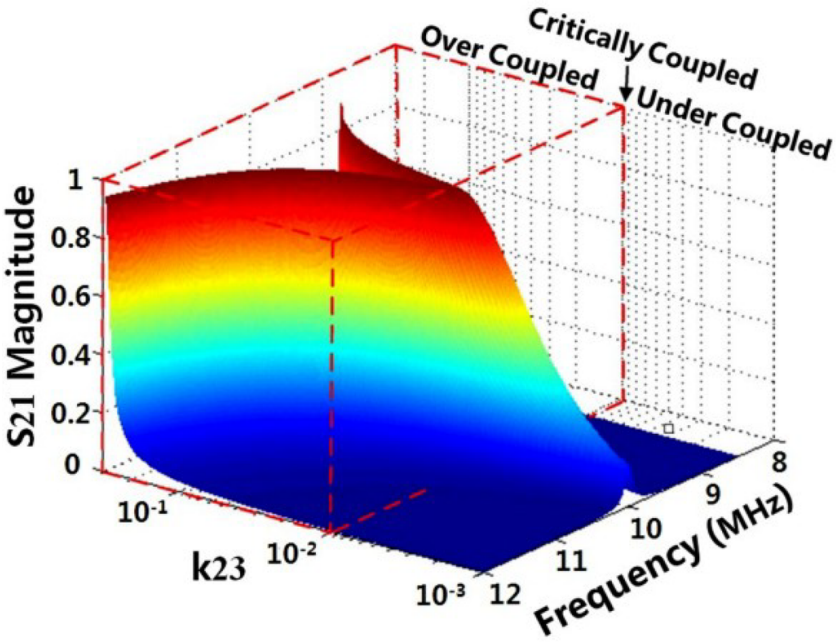

Figure 3.35: Frequency splitting [31]

The voltage ripple caused by delay can be calculated with formula 3.47.

$$dV = \frac{I_C}{C} * t_{delay} \tag{3.47}$$

Inserting the values into this formula gives a voltage ripple of around 8mV, which is a ripple of 0.16%. This is small enough compared to the required 2%.
The downfall of this particular comparator, is that it can handle a maximum supply voltage of 6V. The supply is fed by the voltage over the load, which oscillates around 5V. If something goes wrong, or the delays by the voltage regulator are too large, the load voltage could reach 6V, destroying the comparator. Because of this a voltage regulator is needed between the load voltage and the supply voltage.
In order for the ADCMP361YRJ to perform properly, an appropriately sized pull up resistor, because is has an open collector output, (between Vcc and Vout) and hysteresis resistor (between Vin and Vout) should be connected. A typical value for a pull up resistor is between 1 and 10kΩ. Since this is a higher speed cicuit, a 1kΩ pull up resistor was chosen. A hysteresis resistor of 9.81 kΩ was chosen.

LDO REGULATOR SELECTION

The main specification for the LDO regulator is that its dropout voltage should be as low as possible, in order to keep the power dissipation as low as possible. The MCP1702-5002E/TO from Microchip Technology [34] was chosen for this purpose. It has a maximum voltage drop of 650 mV. The later mentioned gate driver will have an input current, which is the output current of the LDO regulator, of 0.2μA. With formula 3.27 a maximum power dissipation of 0.13 μW is calculated.

GATE DRIVER SELECTION

The only requirements for the gate driver are that its response time is low and that it should be able to make the MOSFETs gate voltage high enough. With these considerations in mind the TPS2829 [35] from Texas Instruments was chosen. This gate driver can handle supply voltages up to 42V, so this supply does not have to be connected to the output of the LDO. The positive-going input threshold voltage at VCC=5 is 4V at maximum. This 4V will always be reached by the output of the comparator, because the LDO regulator has a maximum voltage drop of 0.65V, meaning that the minimum supply voltage of the comparator, and thus output of the comparator will be 5-0.65=4.35V. The input current + the supply+input current of this gate driver is 0.1+0.2=0.3μA, which gives a low power dissipation of 1.5μW. At Vcc=5, it has a delay (propagation time and rise/fall time) of 85ns, for which formula 3.47 gives a caused ripple of 0.13mv, which is sufficiently low.

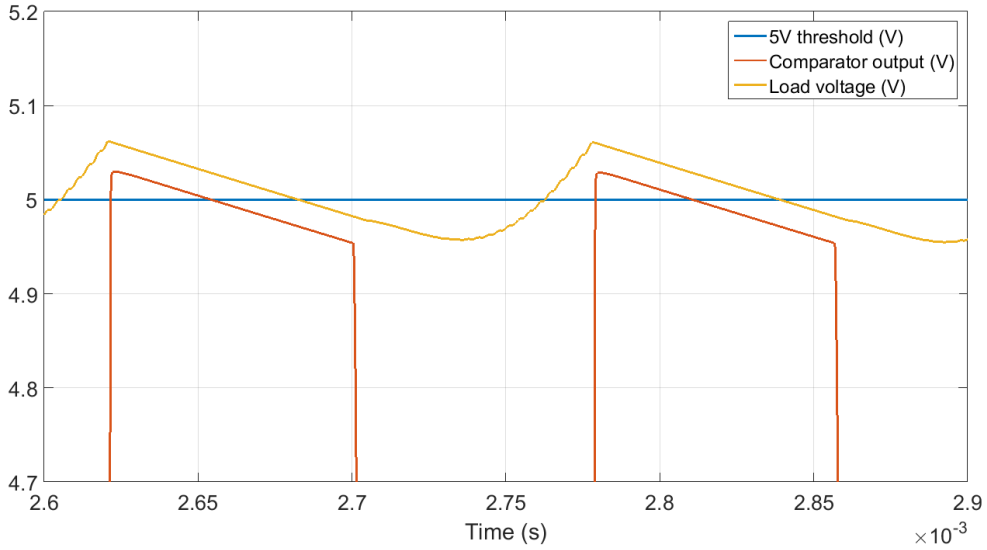

Figure 3.36: Decoupled equivalent circuit

MOSFET SELECTION

The formula for power dissipation in MOSFETs can be found in formula 3.35. The difference in behaviour between these MOSFETs and the MOSFETs used in the rectifier is that these MOSFETs will be turned on and of at a much lower frequency than the ones used in the rectifier. This means that the focus should mainly be on searching for an as low as possible on-resistance. Once again LTspice was used to calculate the approximate RMS current through the MOSFETs. In this case also the switching frequency of the gate driver is calculated by LTspice. The simulated RMS current in steady state is 1.7A and the simulated frequency was around 6kHz. These values are approximations, but they are good enough to select proper components. The simulation used to get these values will be shown in a later section.
The transistors that were chosen are the IRF7842PBF NMOS transistors from Infineon Technologies [36]. Their on-resistance is $5.0m\Omega$ and they have a total gate charge of 33 nC. Their gate-source voltage will be around 5V, since this is what the gate driver is supplied. With these values formula 3.35 gives a power dissipation of 154mW per MOSFET. Energy is only dissipated while the MOSFETs are turned on. Its total delay time is 26 ns, for which formula 3.47 gives a caused ripple of 0.13mV, which is sufficiently low.

SMOOTHING CAPACITOR SELECTION

Lastly the smoothing capacitor parallel to the load has to be selected. Normally this can be done right after the rectifier design. This is done using the formula for current through a capacitor:

Using this formula, the capacitance can be calculated by determining what voltage drop is allowed during the discharge time of the capacitor. During discharge, the capacitor delivers current to the load, so I_C is the load current in this formula. dt Can be determined by calculating the half period of the input wave, since discharge takes place for half a period. This is done with formula 3.48.

$$dt = \frac{1}{2f} \tag{3.48}$$

This gives a dt of about 3.33μs. In the specifications it is mentioned that the maximum allowed ripple voltage is 2%, which is 100mV for a 5V output voltage. With these values formula 3.46 gives a capacitance of 0.333mF. However the ripple voltage of the output is not only determined by the ripple from the rectifier, but mainly by the delays of the voltage regulator. The rectifier ripple can be seen as a ripple on the regulator ripple. This effect is displayed in figure 3.37. In this figure it can be seen that the capacitor size has two effects on the output: The ripple while the capacitor is charging (because this is when the rectifier operates) and the overall ripple voltage. As can be seen in the figure, the ripple while charging the capacitor is very small. Because of this, the most important effect of these two is the latter, since there is a specification for this effect. In formula 3.47 it can be seen that when the capacitance gets larger, the ripple voltage will become lower. Because the charging currents through the capacitor are larger than the discharge currents, $\frac{dV}{dt}$ while charging is larger

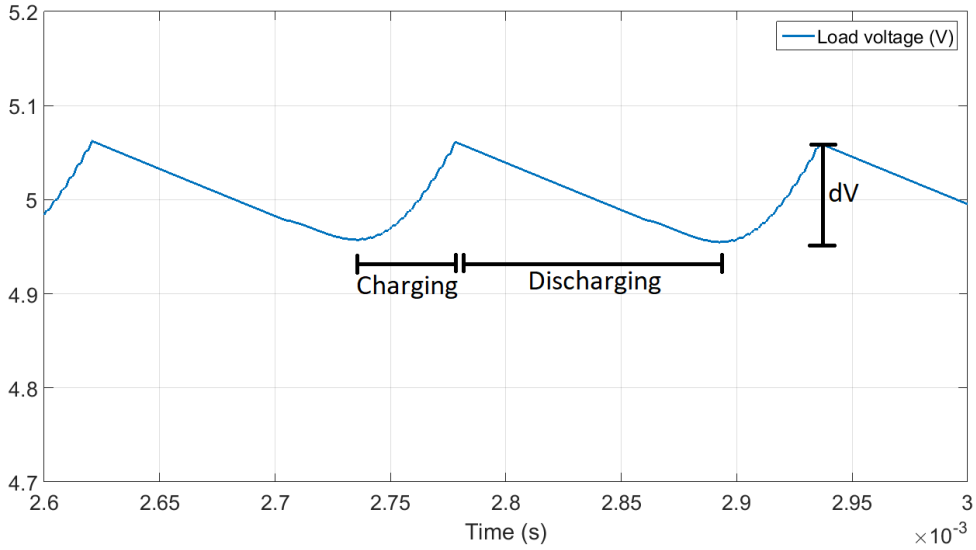

Figure 3.37: Illustration of the total ripple on the output (C=1mF)

than $\frac{dV}{dt}$ while discharging. The discharging current is the load current which is 1A, while in simulation of the whole circuit is can be seen that the charging current is mostly between 1.4A and 1.8A. 2A will be assumed, in order to make a safe calculation.
The ripple voltage is determined by the overshoot and undershoot of the load voltage. The total ripple voltage can be calculated with formula 3.49, which is deduced form formula 3.47.

$$|\Delta V_{total}| = |\Delta V_{discharge}| + |\Delta V_{charge}| = \frac{1A * t_{delay}}{C} + \frac{2A * t_{delay}}{C} = \frac{3 * t_{delay}}{C} \tag{3.49}$$

The calculated total delay of the voltage regulator was around 6μs, but for safety 15μs was assumed. For safety a 1% ripple was selected, which gives a ΔV of 5*0.01=50mV. With these values, formula 3.49 gives a capacitance of 0.9mF. This capacitance was made by connecting two 0.47mF capacitors in parallel, giving a capacitance of 0.47*2=0.94mF, which should suffice. Choosing a larger cap is possible, but this would increase the size and cost of the device. The rectifier ripple will be sufficiently small, because this value is significantly larger than the 0.333mF calculated for the rectifier earlier.
The smoothing capacitor's capacitance will influence the value of the resonance frequency. The 0.94mF capacitor is in series with the 44.5 nF tuning capacitor, for which formula 3.50 gives an equivalent capacitance of 44.498 nF. With formula 3.11 the new oscillation frequency becomes 149.9996kHz, which is such a minor change that it can be neglected.

$$\frac{1}{C_m} = \frac{1}{C_1} + \frac{1}{C_2} \tag{3.50}$$

3.4. FULL CIRCUIT

After the separate sub circuits had been designed and simulated the full receiver circuit could be designed. The schematic of the full circuit and its components are shown in figure 3.38.

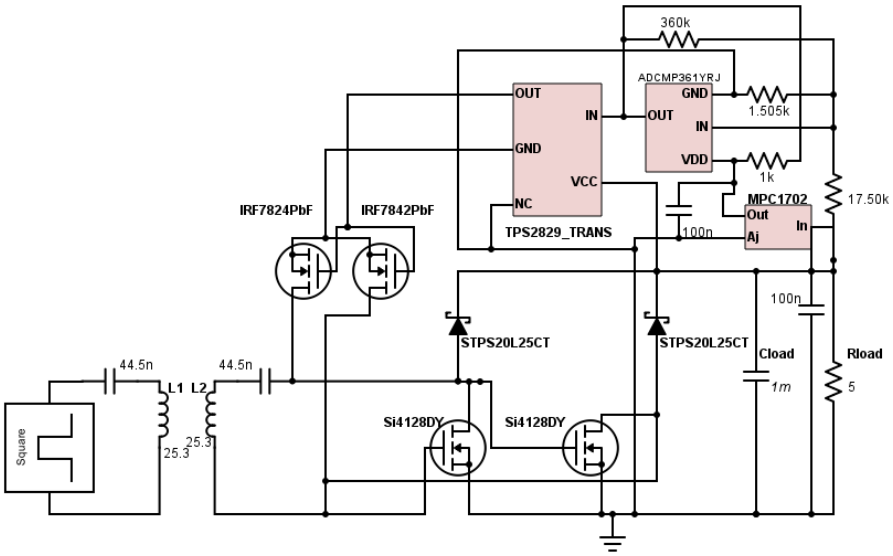

Figure 3.38: Schematic of the receiver

As can be seen, the current from the oscillation circuit either flows through the rectifier and the load or through the shorting MOSFETs.

SIMULATIONS

The full receiving circuit was simulated together with the coupled coils including the transmitter tuning capacitor and a pulse voltage source as transmitter. The coil ESR of 101.5$m\Omega$ and the capacitor ESR of 23.8$m\Omega$ are inserted in LTspice. Since not every component used has an LTspice model, the IRF7842PBF and Si4128DY MOSFETs were replaced with the IRFHS8242pbf, the STPS20L25CT shottky diodes were replaced with the SL43 and the ADCMP361YRJ comparator was replaced with the LT1716 with a 400mV voltage source connected to its inverting input (this source delivered power in the magnitude of pW, so its contribution to the efficiency can be neglected). While these components have comparable specifications, this will influence the simulated circuit. Mainly the values for the efficiency (because of differences in power dissipation) and the ripple voltage (because of difference in delays, formula 3.47) will be affected. In figure 3.39 the load voltage of the entire receiver is shown.

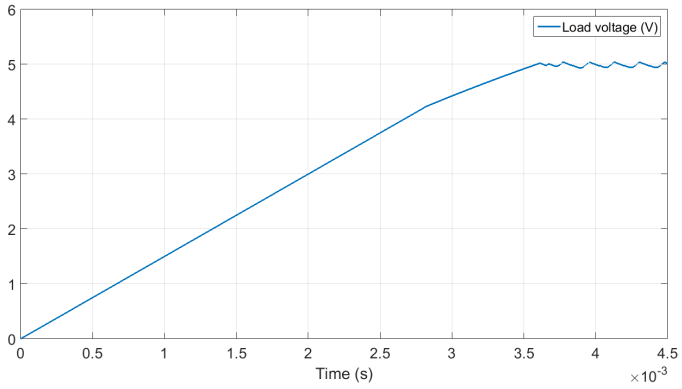

Figure 3.39: Output of the receiver for the first 4.5ms

It can be seen for the first 3.5ms the capacitor is charged up to 5V, after which the output voltage approximates 5V. In figure 3.40 the effect of switching between short circuit mode and rectifier mode on the transmitter current, and thus the needed power. When the gate driver voltage is high, the receiver is in short circuit mode, if it is low, the receiver is in rectifier mode. It can be observed that during short circuit mode,

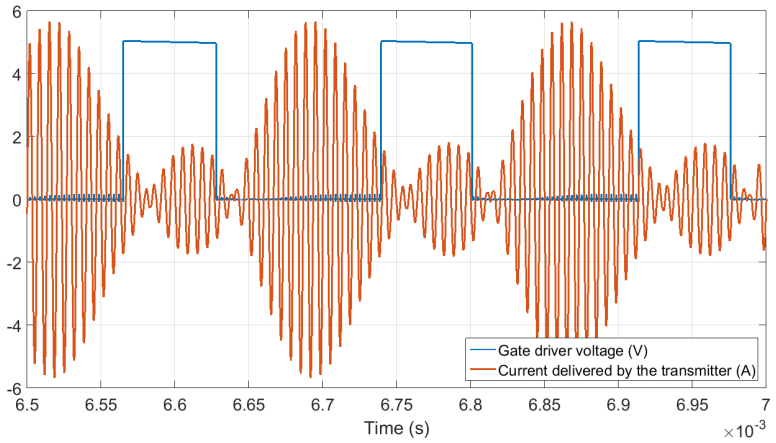

Figure 3.40: The gate driver voltage next to the transmitter current

the transmitter has to deliver less current, which is the sought after effect, since during short circuit mode as little as possible current should be delivered.

Figure 3.41 gives a closer look on the ripple voltage next to the gate voltage of the shorting MOSFETs. This

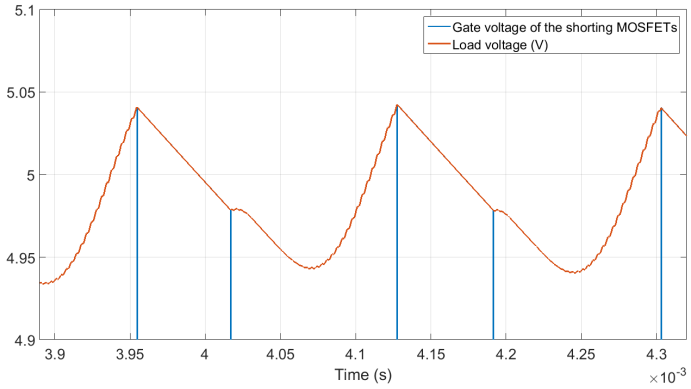

Figure 3.41: Ripple voltage on the output next to the gate voltage of the shorting MOSFETs

figure shows that when the gate signals turn low, meaning when the current will continue flowing through the rectifier, the load voltage does not immediately rise: it first takes another dip before it starts rising. This causes the ripple voltage to be larger than the expected 50mV (1%). This is caused by an effect that can be seen in figure 3.42.

This figure shows that when the receiver has just turned back to rectifier mode (when the gate driver voltage turns low), the amplitude of the receiver coil current needs some time to increase back to its maximum value. Because of this, for a short period after rectifier mode has begun, the smoothing capacitor still isn't receiving any charge, meaning that the load voltage (and thus smoothing capacitor voltage) will continue to drop for this period of time.

This phenomenon occurs because the circuit needs some time before it has adjusted to its new configuration. The amount of time that this takes is dependent on the time constant τ of the circuit. The relation between time constant and the percentage of the steady state voltage is shown in figure 3.43. The figure shows that after about 5τ the circuit will have reached steady state. τ is dependent on the quality factor Q of the system. Formula 3.45 is the formula for the Q factor of a series RLC circuit. To make an estimation for the time

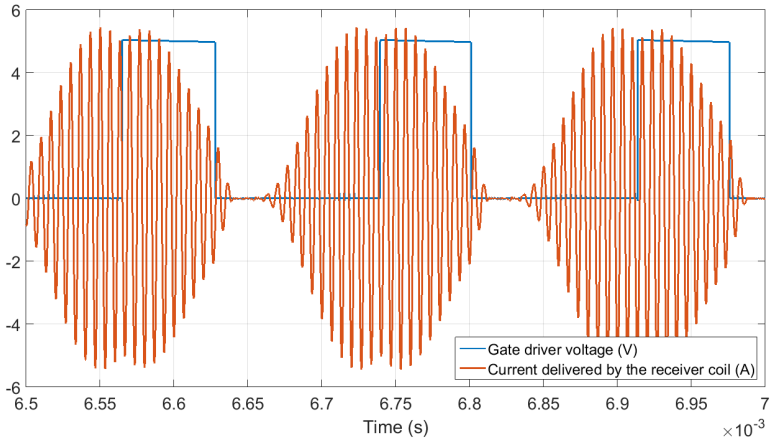

Figure 3.42: The gate driver voltage next to the receiver coil current current

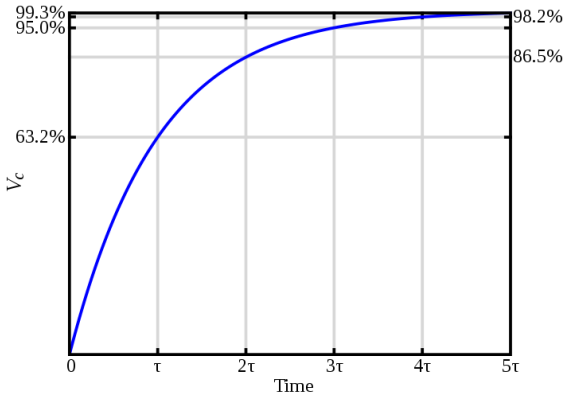

Figure 3.43: Relation between time constant and voltage amplitude [37]

constant of the receiver in rectifier mode, a resistance of 5.5 is assumed. 3.45 then gives a Q factor of 4.34. Formula 3.51 gives the time constant as a function of the Q factor.[38]

$$\tau = \frac{2Q}{2\pi f_{osc}} \tag{3.51}$$

From this formula it follows that τ is around 9.2μs. This mean that after 5*9.2=46μs (5τ) the circuit should be in steady state. This estimation somewhat resembles figure 3.42.

The simulation gives a receiver efficiency (resonant circuit power/load power) of 89.9% once it has reached steady state. The efficiency of the receiver + the coils (transmitter power/load power) with a coupling of 0.1 (around 3cm) is 70.1%. A ripple voltage of 87.43 mV is measured, which is 1.75%.

3.5. SAFETY

There are certain safety standards that a wireless power transfer device has to adhere to. The main factor of importance is human safety: the magnetic field and electric components should not be harmful to the human body.
In the standards NPR-IEC/TR 62869 'activities and considerations related to wireless power transfer (WPT) for audio, video and multimeadia systems and equipment' [39], IEC TR 62905:2018 'Exposure assessment methods for wireless power transfer systems' [40] and several EMC standards, it was found that at frequencies up to 150kHz, and at the power this device operates at, there are no safety or other concerns that have to be accounted for.

4

PROTOTYPE AND RESULTS

A prototype is created to validate the circuit simulations done in ltspice and to evaluate the final efficiency of this WPT-system. This chapter will explain how testing of the single blocks and the complete system is done. It will first introduce the final prototype in section 4.1. The efficiency and power losses in the air coupled coils, the rectifier and the voltage regulator will be described in section 4.3. Then section 4.4 will explain and show the combined efficiency of the air-coupled coils and the receiver. Finally, section 4.5 will describe the performance of this complete WPT-system, the combined efficiency of the transmitter, air coupled coils and the receiver.
The measurements were done with the Tektronix PWS4205 Programmable DC Power Supply, Fluke 177 True RMS Multimeter and Tektronix TDS2022C two channel digital storage oscilloscope.

4.1. PROTOTYPE

Figure 4.1 shows the top and bottom side of the complete prototype of the receiver side. The tuning capacitor is placed close to the coil, there are six capacitors in parallel to create a capacitance of 45.9nF, which results in a resonance frequency of 147.6kHz.
The other AC components are also placed near the coil, to keep the losses due to the AC resistance of the connecting wires as low as possible. This includes the two MOSFETs and the diodes of the rectifier, which are placed between the coil and the large load capacitor. Next to the load capacitance the load resistance can be found. The voltage regulator is placed just as in the schematics in figure 3.38 above the load, with again the MOSFETs close to the other AC components. Placing them further away from the coil will result in a larger AC resistance in the wires, something that needs to be prevented as mentioned in 3.3.3. The other side of figure 4.1 shows the connections between the components with the coil attached.

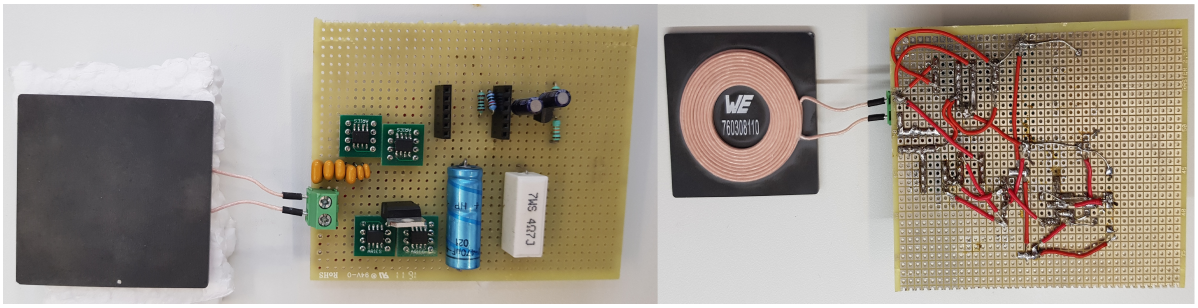

Figure 4.1: Top and bottom view of the receiver side

4.1.1. COMPLETE SYSTEM OVERVIEW

Figure 4.2 shows both prototypes combined forming a wireless power transfer system, with the receiver on the right side, the transmitter on the left side and the air-coupled coils between them. The air-coupled coils are 20mm separated by expanded polystyrene, a non-conducting material.

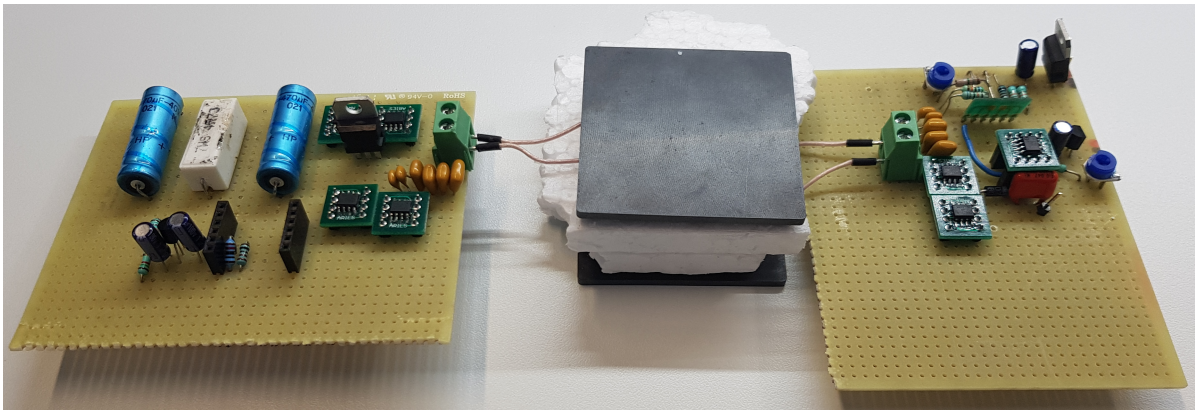

Figure 4.2: Combined system of the transmitter and the receiver

4.2. MEASUREMENT METHODOLOGY

Measurements are done using a probe and the TDS2022C oscillator. The wave forms are exported to Matlab. Matlab is then used to plot the signals and to derive current or power in different blocks. The coils and capacitors have been measured with a LCR Meter HC8018, to make sure that the capacitance and inductance variance was accounted for in both the receiver and the transmitter.

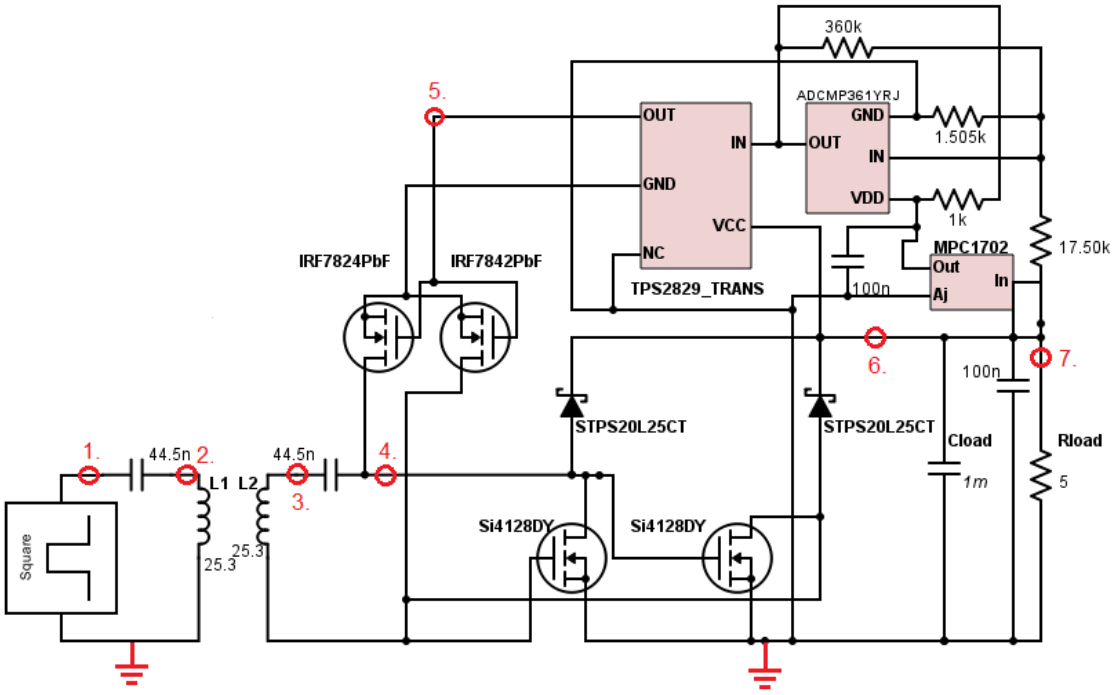

Figure 4.3: Combined system of the transmitter and the receiver

Seven dots in figure 4.3 are the places were the probes are attached to do the measurements which are included in this report. There will be referred back to this figure in this section to give a better view of the measurements done on this WPT-system.

4.3. SINGLE BLOCK RESULTS

4.3.1. AIR COUPLED COILS

The measured inductance value of the coils was 25.3μH. The coupling between the coils over the distance is shown in figure 4.4a. The coupling is calculated by leaving the receiving coils as an open terminal. The mutual inductance can then be calculated with equation 3.3. The data that was used to make this figure can be found in Appendix A.2.1. The coupling is around 0.1 at a distance of 25mm, as can be seen in figure 4.4a. Sheets of paper are used to determine the spacing between the coils as shown in figure 4.4b. Five sheets of paper result in a distance of about 0.5 mm, a light press on the top coil ensures that no air is trapped in between the paper sheets. The signals form both coils can be seen in the oscilloscope, while the transmitting coil is powered using an amplifier at a fixed frequency.

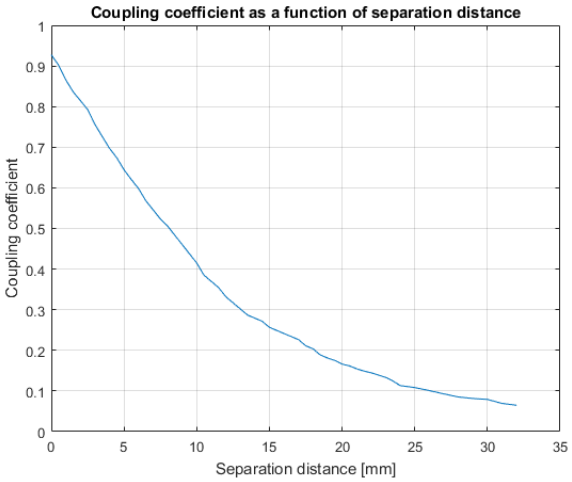

(a) Coupling between two coils over the separation distance

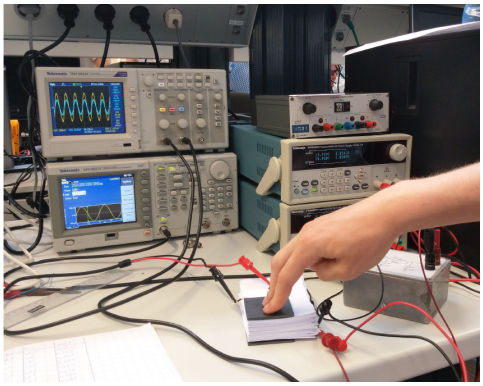

(b) Measurement setup for coupling coefficient calculations

Figure 4.5 shows the input voltage of the resonant circuit and the voltage over the tuning capacitor on the transmitter side. The voltage over the resonance circuit approaches a square wave, because of the smoothing capacitor of the rectifier. The input voltage of the resonant circuit is measured with 1. to the ground and the voltage over the tuning capacitor is measured with 1. and 2. in figure 4.3. The voltage over the capacitor is used to calculate the current through the resonance circuit of the transmitter by:

$$I = \frac{V}{Z} = V \cdot (j \cdot \omega \cdot C) \tag{4.1}$$

Both figures 4.5 and 4.6 are generated with the Matlab code from Appendix A.2.

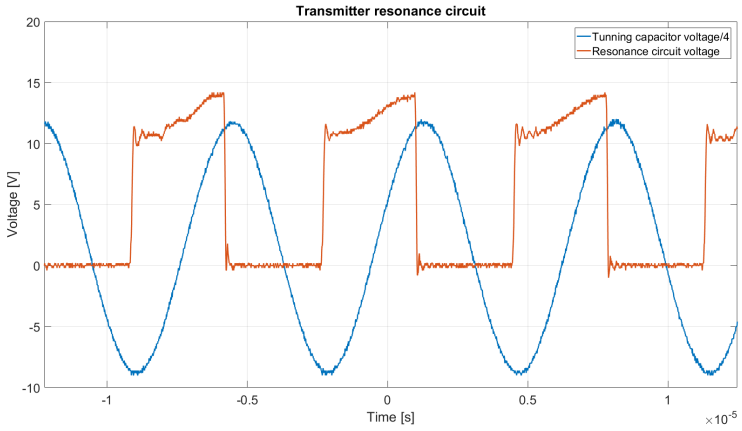

Figure 4.5: Transmitter input voltage of the resonance circuit and voltage over the tuning capacitor

The power that goes into the transmitting coil can be determined by:

$$P = V_{RMS} \cdot I_{RMS} \tag{4.2}$$

V_{RMS} is the voltage over the resonance circuit in the transmitter and I_{RMS} can be calculated with equation 3.35. The power that is delivered to the resonant circuit is then 6.69 W. The calculated peak current was 1.66A.

Figure 4.6 shows the input voltage of the resonant circuit and the voltage over the tuning capacitor on the receiver side, which is used to calculate the current through the resonance circuit of the receiver with equation 4.1. The voltage over the resonant circuit is measured with 3. to the ground and the voltage over the tuning capacitor is measured with 3. and 4. in figure 4.3.

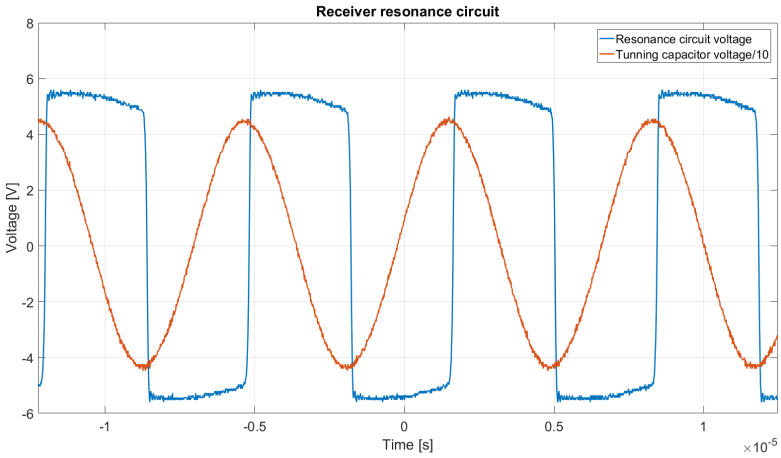

Figure 4.6: Receiver output voltage of the resonance circuit and voltage over the tuning capacitor

The power delivered by the air coupled coils can be calculated with:

$$P = V_{RMS} \cdot I_{RMS} \tag{4.3}$$

V_{RMS} is the voltage over the resonance circuit in the receiver and I_{RMS} can be calculated with equation 3.35. The power that is delivered by the resonant circuit is then 6.17 W. The calculated peak current through the receiving resonant circuit was 1.99A. The efficiency of the resonant circuit with a coil distance of 2cm can be calculated by:

$$\eta_{maximum} = \frac{P_{output}}{P_{input}} * 100\% = \frac{6.17W}{6.69W} * 100\% = 92.2\% \tag{4.4}$$

In figure 4.6 it can also be seen that the resonant circuit voltage is a square wave form instead of a sinus. This is caused by the smoothing capacitor parallel to the load: the voltage over this capacitor can not change rapidly, which is seen by the receiver coil.

4.3.2. RECTIFIER

Figure 4.7 shows the output voltage of the rectifier, which is measured with a probe on 6. in figure 4.3. The voltage "spikes" that could be caused by probe errors. The measured voltage ripple was surprisingly large: around 200 mV or 4%.

4.3.3. VOLTAGE REGULATOR

Figure 4.8 shows the gate voltage of both MOSFETs used to short circuit the resonant circuit. The gate voltage is measured with 5. and the load voltage with 7., both in figure 4.3. The gate voltage of the MOSFETs becomes high when the load voltage exceeds 5V until the load voltage drops below 5V again. The load voltage could now be fixed at 5V, with a ripple of about 6 – 7%. Unfortunately the size of the ripple exceeds the requirement of 2%. This is caused by a longer propagation delay by the comparator than expected, and by the rectifier ripple being larger than expected. Sadly no comparator with built in voltage reference could be found that was faster than the one that is used.

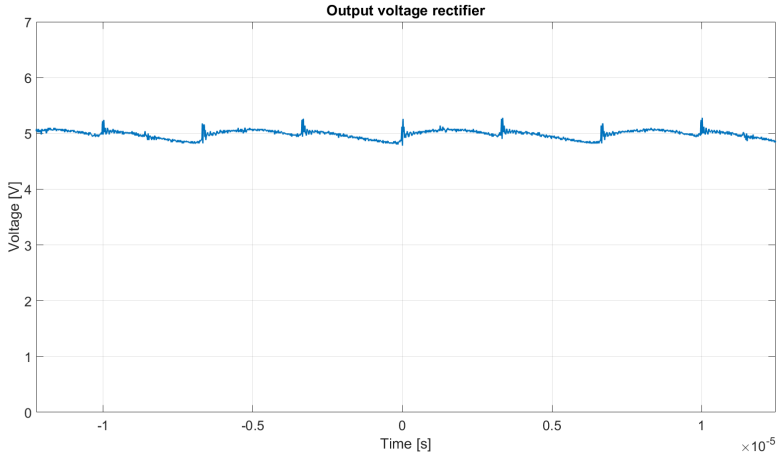

Figure 4.7: Rectifier output voltage

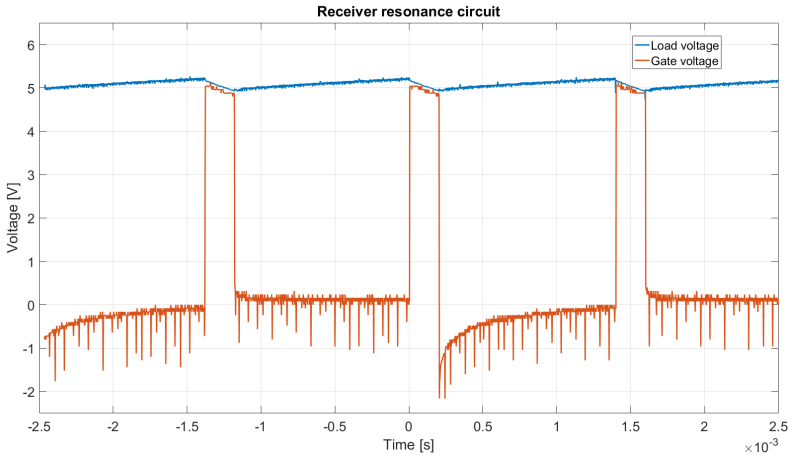

Figure 4.8: Load voltage and gate voltage

4.4. RECEIVER AND RESONANT CIRCUIT EFFICIENCY'S

Some the losses in the resonant circuit are from the equivalent series resistances in both resonant circuits. These losses are calculated with equation 4.5.

$$
\begin{aligned}
P = I_{rms}^2 \cdot R_{series} = \frac{I_{peak}^2}{2} \cdot R_{series} \\
\Rightarrow \\
P_{transmitter} = \frac{1.66^2}{2} \cdot 0.1163 = 160mW \\
P_{receiver} = \frac{1.99^2}{2} \cdot 0.1163 = 230mW \\
P_{Rseries} = 160 + 230 = 390mW
\end{aligned}
\tag{4.5}
$$

The losses in the magnetic field are then approximately $(6690mW - 6170mW) - 390mW = 520mW - 390mW = 130mW$. The output power is also known, 5W, the losses in the rectifier can be found by: $6.17W - 5W = 1.17W$.

4.5. COMPLETE WPT-SYSTEM RESULTS

This subsection combines the product of this thesis with the other thesis about wireless power transfer as mentioned in the preface. Figure 4.9a shows the input power of the transmitter for different distances and different frequencies around the resonance frequency. The input power is calculated with the input current and voltage from the DC power supply with equation 4.6, while a steady 5V output is measured with a multimeter.

$$P = U * I \tag{4.6}$$

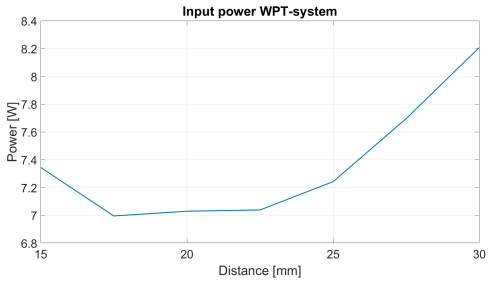

(a) Supply power transmitter over distance

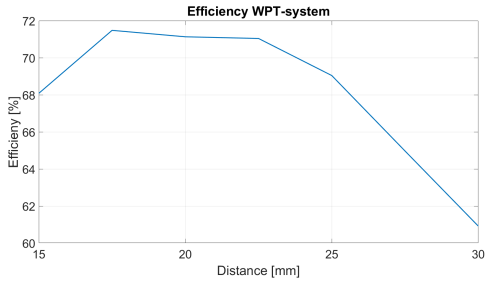

(b) Total efficiency over distance

The smallest input power needed for an 5W output is 6.99W, the maximum efficiency is given by:

$$\eta_{maximum} = \frac{P_{output}}{P_{input}} * 100\% = \frac{5W}{6.99W} * 100\% = 71.5\% \tag{4.7}$$

The efficiency's over multiple distances are shown in figure 4.9b. The maximum efficiency is obtained with the resonance frequency on a distance of 17.5 mm. The efficiency drops below the limit from a distance larger than 30 mm, no result could be obtained on a distance lower than 15 mm.
The rectifier efficiency can then be calculated by:

$$\eta_{maximum} = \frac{P_{output}}{P_{input}} * 100\% = \frac{5W}{6.17W} * 100\% = 81.0\% \tag{4.8}$$

The previous results are obtained given the fact that the output voltage is always 5V with a coil distance of 2cm. Adjusting the output voltage, and thereby the output power, could result in a higher efficiency, for example due to the diode voltage drops that become less significant. This can be seen in figure 4.10.

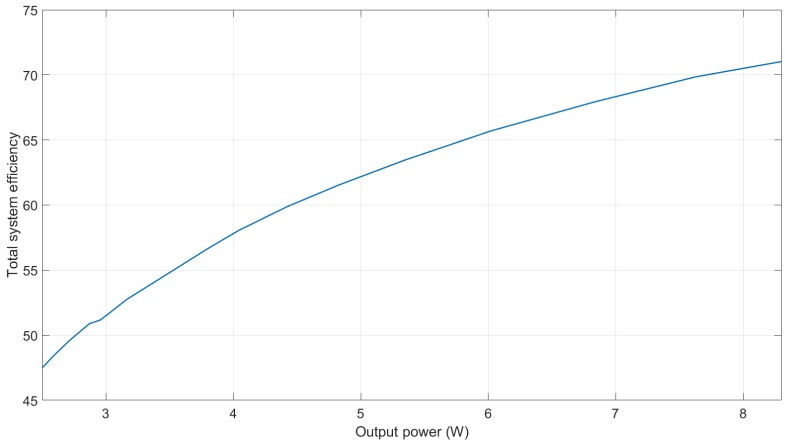

Figure 4.10: Efficiency with different output values

5

Conclusion

The purpose of this project was to design a wireless power transfer system for hand-held mobile devices, with an overall efficiency of at least 60% at a maximum possible distance. The air coupled coils and the receiver side of this system are examined in this thesis.

5.0.1. Conclusion

First the air coupled coils needed to be chosen or designed. Designing a coil for this special purpose could improve the overall performance, but it became clear that building the exact model as simulated was too difficult and the consequences of small changes are impossible to predict. Therefore two coils from Würth Elektronik (760308110)[17] were ordered form an external company. Their large self-inductance and high quality factor were decisive.

The AC signal from the resonance circuit needed to be rectified to get a DC output voltage over the load. Multiple implementations were considered, starting with the choice between a half bridge rectifier or a full bridge rectifier. Resistive components in a half bridge will dissipate twice as much energy as they will in a full bridge configuration. Because of this and the fact that a full bridge can function with a smaller smoothing capacitor, the full bridge setup was chosen. Since MOSFETs have a lower power loss than diodes it would be ideal to replace every diode in the full bridge rectifier with MOSFETs. A number of attempts were made at achieving this setup, but did not succeed. A much simpler rectifier design has been implemented, a full bridge which uses two schottky diodes and two MOSFETs. This implementation is not as efficient as the diode less rectifier, but it is still a big improvement compared to the standard full bridge rectifier with 4 diodes. Two schottky diodes from STMicroelectronics (TPS20L25CT) and two MOSFETs from VISHAY (Si4128DY) were chosen.

And finally a DC-DC converter needed to be implemented to maintain a steady 5W output. Because of the variable output, two buck-boost converters were considered. The ADP2504-5.0 and the LTC3114-1.0 are both high efficiency step-up/step-down converters. Even though single simulations were promising, complete system simulations did not fulfill the expectations. The input capacitor would burn in both cases when this system was built without feedback to control the input power. Therefore a voltage regulator, which shorts the resonance circuit when the output power exceeds 5W, has been designed. A gate driver (TPS2829_TRANS) increases the output signal of a comparator (ADCMP361YRJ) with an internal 400mV reference voltage to control two MOSFETs (IRF7824PbF), which shorts the resonance circuit. This implementation controls the input power of the transmitter, it resulted in a higher simulated efficiency. Unfortunately it did not work properly in the prototype before the deadline of this thesis. Measurements taken with the voltage regulator deactivated, result in a varying output voltage as a function of distance and alignment as is to be expected.

The combined system of transmitter and receiver achieved the main goals of the project, a 5W output with an overall efficiency of at least 60%. The maximum efficiency reached at a distance of 17.5 mm is 71.5%. The requirements are still achieved at a distance of 30 mm.

5.0.2. RECOMMENDATIONS

First the voltage regulator must be improved or replaced to remove or decrease the large ripple. More research in a DC-DC converter and in the rectifier could make it even more efficient. Future work could also be done to improve the maximum charging distance at the same efficiency, by for example improving the air coupled coils and design them for this purpose only. Also communication between the transmitter and receiver could be used to make sure the device always operates at the perfect resonant frequency, like is done in Qi[5] charging. At last, a better combination of components might result in a stronger power transfer.

6

Discussion

Even though the specifications were mostly achieved, there are some lessons that were learned. A frequently occurring situation was that a certain value or component was chosen, on which the rest of the circuit was based. When this component or value is later changed however, other parts of the system have to change with it. This caused some subcircuits and components not maximally compatible, causing the final result not completely ideal.
For example the operating frequency. It was found out that the 150kHz value was calculated for a coupling of 0.1, but since the system has to work at different levels of coupling, it is likely that this 150kHz is not the ideal value.
Another example are the MOSFETs used in the rectifier. Due to some design changes since the MOSFETs were ordered, they do not have the ideal specifications in order to have an as high as possible efficiency.
During the design process there were some goals that were not achieved. The main example of this was the design of a diode less rectifier. The designed circuits were deemed to complex and unreliable to be implemented in the circuit. Maybe if more time had been available, this goal would have been achieved, but for now the current rectifier design operates sufficiently.
A buck/boost converter could also be added at the output (in combination with the custom voltage regulator) to reduce the ripple voltage, but this would also reduce the total efficiency. Also the measured ripple voltage was higher than expected. Because no faster comparator with built in reference was found, this could be solved by using a low drop-out voltage regulator in order to create a built in reference voltage. When this is done, a normal, faster comparator could be used, significantly reducing the ripple voltage. Because barely any current flows into the input of comparators, the LDO regulator would dissipate very little power.

A

APPENDIX

A.1. MATLAB CODE

A.1.1. EFFICIENCY CALCULATIONS

PowerResonantCircuit.m

```
clear all
close all

Ploss = zeros(10,4);

%Starting values
f = 50e3:50e3:500e3;
omega = f.*2.*pi;
L = 24e-6;
C = round(1 ./ (omega.^2 .* L), 12);
eff = 0.9; %receiver efficiency

%Rectifier resitance and power calculations
Rrect_load = 5;
Rrect_loss = 5 / eff - 5;
Prect = 5 / eff;

%% Stage 1: Frequency dependent power transfer

%Coil & Tuning Capacitor ESR
Rseries = 0.1;

for i = 1:4
    %Multiple itterations for different couplings
    k = 0.06 + 0.02 * i;
    legendStrings{i} = num2str(k,'k = %g');
    M = k * L;

    %Total receiver resistance calculation
    R = Rrect_load + Rrect_loss + Rseries;
    P = R;

    %Power loss
    Ploss(:,i) = Rseries .* P .* (1./R + R./(omega.^2.*M.^2));
end

figure(1)
subplot(121)
grid on
hold on
plot(f/1000, Ploss)
axis([50 500 0 10])
title('Power Loss in Resonant Circuit')
xlabel('Frequency [kHz]')
ylabel('Power Loss [W]')
legend(legendStrings)

subplot(122)
grid on
hold on
plot(f'/1000, Prect./(Prect+Ploss))
axis([50 500 0.5 1])
title('Efficiency in Resonant Circuit')
```

```
xlabel('Frequency [kHz]')
ylabel('Efficiency')
legend(legendStrings, 'Location', 'southeast')

printpdf2('eff1.pdf');

%% Stage 2: Including a frequency dependent equivalent series resistance

%Q factors and Dissipation Factor as found in the datasheet
Q = [115 200 235 230 200 180 160 150 135 125 115 110 105 100  95  90  88  85  80  78];
DF = 0.001;

%ESR calculation
Rseries = ( omega .* L ./ Q(1:10) ) + ( DF ./ (omega .* C) );

for i = 1:4
    %Multiple itterations for different couplings
    k = 0.06 + 0.02 * i;
    legendStrings{i} = num2str(k,'k = %g');
    M = k * L;

    %Total receiver resistance calculation
    R = Rrect_load + Rrect_loss + Rseries;
    P = R;

    %Power loss
    Ploss(:,i) = Rseries .* P .* (1./R + R./(omega.^2.*M.^2));
end

figure(2)
subplot(121)
grid on
hold on
plot(f/1000, Ploss)
axis([50 500 0 10])
title('Power Loss in Resonant Circuit')
xlabel('Frequency [kHz]')
ylabel('Power Loss [W]')
legend(legendStrings)

subplot(122)
grid on
hold on
plot(f'/1000, Prect./(Prect+Ploss))
axis([50 500 0.5 1])
title('Efficiency in Resonant Circuit')
xlabel('Frequency [kHz]')
ylabel('Efficiency')
legend(legendStrings, 'Location', 'southeast')

printpdf2('eff2.pdf');
```

A.2. MEASUREMENTS

finalresults1.*m*

```
clear all;
close all;
clc;

Fs = 100e6;
f = 146.7e3;
quarter = Fs/f/4;
omega = f * 2 * pi;
L = 24e-6;
C = round(1 ./ (omega.^2 .* L), 12);

load receiver1.mat
load receiver2.mat
load receivertime.mat

t = ReceiverCH3;
Vout = ReceiverCH1;
Vc = ReceiverCH2./10;

plot(t,Vout)
hold on
plot(t,Vc)
grid on
axis([-1.224e-5 1.247e-5 -6 8])
xlabel('Time [s]')
ylabel('Voltage [V]')
title('Receiver resonance circuit')
```

```
legend('Resonance circuit voltage','Tunning capacitor voltage/10')
set(findall(gca, 'Type', 'Line'),'LineWidth',2);
set (gca, 'fontsize', 20);
```

A.2.1. COIL MEASUREMENTS

Table A.1: Measurements of the coupling between two coils

distance (mm)	V in	V out
0	1,1	1,02
0,5	1,1	0,992
1	1,1	0,952
1,5	1,1	0,92
2	1,1	0,896
2,5	1,09	0,864
3	1,09	0,824
3,5	1,09	0,792
4	1,09	0,76
4,5	1,08	0,728
5	1,08	0,696
5,5	1,07	0,664
6	1,07	0,64
6,5	1,07	0,608
7	1,07	0,584
7,5	1,07	0,56
8	1,06	0,536
8,5	1,06	0,512
9	1,06	0,488
9,5	1,06	0,464
10	1,06	0,44
10,5	1,06	0,408
11	1,06	0,392
11,5	1,06	0,376
12	1,06	0,352
12,5	1,06	0,336
13	1,06	0,32
13,5	1,06	0,304
14	1,06	0,296
14,5	1,06	0,288
15	1,06	0,272
15,5	1,06	0,264
16	1,06	0,256
16,5	1,06	0,248
17	1,06	0,24
17,5	1,06	0,224
18	1,06	0,216
18,5	1,06	0,2
19	1,06	0,192
19,5	1,05	0,184
20	1,06	0,176
20,5	1,05	0,17
21	1,06	0,164
21,5	1,06	0,158
22	1,05	0,152
22,5	1,05	0,146
23	1,05	0,14
23,5	1,06	0,132
24	1,06	0,12
25	1,06	0,115
26	1,06	0,107
27	1,06	0,0984
28	1,06	0,0904
29	1,06	0,0864
30	1,06	0,084
31	1,06	0,0736
32	1,06	0,0688

BIBLIOGRAPHY

[1] J. van der Velden and L. Marting, "Wireless charger for hand-held mobile devices," June 2018.

[2] X. Lu, P. Wang, D. Niyato, D. I. Kim, and Z. Han, "Wireless charging technologies: Fundamentals, standards, and network applications," *IEEE Communications Surveys Tutorials*, vol. 18, no. 2, pp. 1413–1452, Secondquarter 2016.

[3] A. K. RamRakhyani, S. Mirabbasi, and M. Chiao, "Design and optimization of resonance-based efficient wireless power delivery systems for biomedical implants," *IEEE Transactions on Biomedical Circuits and Systems*, vol. 5, no. 1, pp. 48–63, Feb 2011.

[4] D. van Wageningen and T. Staring, "The qi wireless power standard," in *Proceedings of 14th International Power Electronics and Motion Control Conference EPE-PEMC 2010*, Sept 2010, pp. S15–25–S15–32.

[5] "https://www.wirelesspowerconsortium.com/."

[6] "https://www.airfuel.org/."

[7] S. Y. R. Hui, W. Zhong, and C. K. Lee, "A critical review of recent progress in mid-range wireless power transfer," *IEEE Transactions on Power Electronics*, vol. 29, no. 9, pp. 4500–4511, Sept 2014.

[8] D. Liu and S. V. Georgakopoulos, "Cylindrical misalignment insensitive wireless power transfer systems," *IEEE Transactions on Power Electronics*, 2018.

[9] K. S. Nikita, *Handbook of Biomedical Telemetry*, 2014, PUBLISHER = WILEY, PAGE = 175, NOTE = First edition.

[10] D. Xu, S. Yin, and D. Wang, "Analysis of frequency splitting phenomena for magnetic resonance wireless power transfer systems," in *2017 Chinese Automation Congress (CAC)*, Oct 2017, pp. 2614–2618.

[11] X. Li, X. Dai, Y. Li, Y. Sun, Z. Ye, and Z. Wang, "Coupling coefficient identification for maximum power transfer in wpt system via impedance matching," in *2016 IEEE PELS Workshop on Emerging Technologies: Wireless Power Transfer (WoW)*, Oct 2016, pp. 27–30.

[12] H. Li, J. Fang, S. Chen, Y. Tang, and K. Wang, "A pulse density modulation method for zvs full-bridge converters in wireless power transfer systems," in *2018 IEEE Applied Power Electronics Conference and Exposition (APEC)*, March 2018, pp. 3143–3148.

[13] T. Koyama, T. Honjo, M. Ishihara, K. Umetani, and E. Hiraki, "Simple self-driven synchronous rectifier for resonant inductive coupling wireless power transfer," in *2017 IEEE International Telecommunications Energy Conference (INTELEC)*, Oct 2017, pp. 363–368.

[14] H. Wenshan, Y. Lingsong, L. Zhiwei, and Y. Hui, "Loss analysis and improvement of all parts of magnetic resonant wireless power transfer system," in *2015 Chinese Automation Congress (CAC)*, Nov 2015, pp. 2251–2256.

[15] S. Chopra and P. Bauer, "Analysis and design considerations for a contactless power transfer system," in *2011 IEEE 33rd International Telecommunications Energy Conference (INTELEC)*, Oct 2011, pp. 1–6.

[16] M. H. Tooley, *Electronic Circuits*. Nownes, 2006, third edition.

[17] *WE-WPCC Wireless Power Charging Transmitter Coil*, Würth Elektronik, rev. 001.009.

[18] H. A. Wheeler, "Formulas for the skin effect," *Proceedings of the IRE*, vol. 30, no. 9, pp. 412–424, Sept 1942.

[19] L. Jinliang, D. Qijun, H. Wenshan, and Z. Hong, "Research on quality factor of the coils in wireless power transfer system based on magnetic coupling resonance," in *2017 IEEE PELS Workshop on Emerging Technologies: Wireless Power Transfer (WoW)*, May 2017, pp. 123–127.

[20] H. Li, X. Yang, K. Wang, and X. Dong, "Study on efficiency maximization design principles for wireless power transfer system using magnetic resonant coupling," in *2013 IEEE ECCE Asia Downunder*, June 2013, pp. 888–892.

[21] "https://www.elprocus.com/full-wave-bridge-rectifier-versus-center-tapped-full-wave-rectifier."

[22] "https://www.elprocus.com/bridge-rectifier-circuit-theory-with-working-operation/."

[23] "https://commons.wikimedia.org/wiki/file:diode_mosfet.svg."

[24] G. Lakkas, "Mosfet power losses and how they affect power-supply efficiency," http://www.ti.com/lit/an/slyt664/slyt664.pdf.

[25] "http://nl.farnell.com/."

[26] *LOW DROP POWER SCHOTTKY RECTIFIER*, STMicroelectronics, rev. 2003.

[27] *N-Channel 30-V (D-S) MOSFET*, Vishay, rev. 08-Feb-17.

[28] *UCC27714 High-Speed, 600-V High-Side Low-Side Gate Driver with 4-A Peak Output*, Texas Instruments, rev. 2017.

[29] *600mA/1000mA, 2.5MHz Buck-Boost, DC-DC Converters*, Analog devices, rev. D.

[30] *40V, 1A Synchronous Buck-Boost DC/DC Converter with Programmable Output Current*, Linear technology, rev. B.

[31] Z. W. Xuezhe Wei and H. Dai, "A critical review of wireless power transfer via strongly coupled magnetic resonances," Sept 2014.

[32] "http://www.ee.bgu.ac.il/~intrlab/lab_number_7/two%20inductively%20coupled%20rlc%20circuits.pdf."

[33] *Single 0.275% Comparator and reference with Dual Polarity Outputs*, Analog devices, rev. B.

[34] *250 mA Low Quiescent Current 5V LDO Regulator*, Microchip Technology, rev. 09-14-05.

[35] *Single-channel High-speed MOSFET Driver*, Texas Instruments, rev. october 2002.

[36] *HEXFET Power MOSFET*, Infineon Technologies, rev. 7/8/2014.

[37] "https://commons.wikimedia.org/wiki/file:series_rc_capacitor_voltage.svg."

[38] "https://math.dartmouth.edu/ ahb/scia49/q.pdf."

[39] I. E. Commision, "Iec tr 63167:2018 assessment of contact current related to human exposure to electric, magnetic and electromagnetic fields," June 2018.

[40] N. S. Institute, "Iec tr 62905:2018 'exposure assessment methods for wireless power transfer systems," July 2013.